

AD-A054 252

RENSSELAER POLYTECHNIC INST TROY N Y DEPT OF MECHANICS--ETC F/G 11/6
A NONLINEAR UNIAXIAL INTEGRAL CONSTITUTIVE EQUATION INCORPORATING--ETC(U)
FEB 78 E P CERNOCKY, E KREML

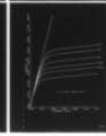
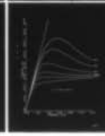
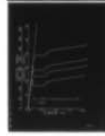
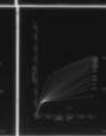
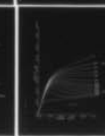
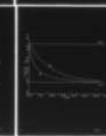
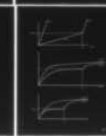
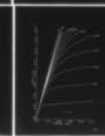
N00014-76-C-0231

UNCLASSIFIED

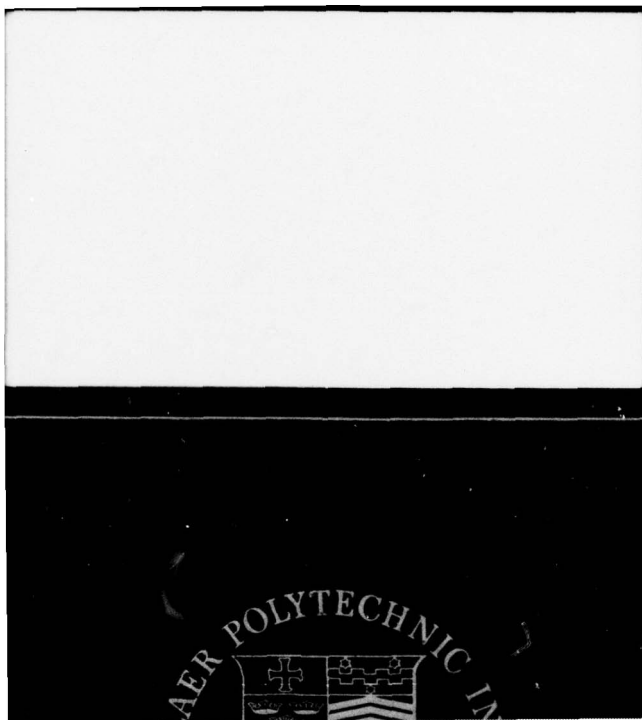
RPI-CS-78-1

NL

1 OF 1
AD
A054252



END
DATE
FILMED
6 -78
DDC



FOR FURTHER TRAN

AD A 054252

6 A NONLINEAR UNIAXIAL INTEGRAL CONSTITUTIVE
EQUATION INCORPORATING RATE EFFECTS,
CREEP, AND RELAXATION,

10 E. P. / Cernocky ~~and~~ E. / Kreml
Department of Mechanical Engineering,
Aeronautical Engineering & Mechanics
Rensselaer Polytechnic Institute
Troy, New York 12181

AD NO.
DDC FILE COPY

15 Contract No. N00014-76-C-0231

14 Report No. RPI-CS-78-1

11 Feb 1978

12 43 p.

ACCESSION FOR	
NTIS	White Section <input checked="" type="checkbox"/>
DDC	Buff Section <input type="checkbox"/>
UNANNOUNCED	<input type="checkbox"/>
JUSTIFICATION	
<i>letter on file</i>	
BY	
DISTRIBUTION AVAILABILITY CODE	
BIBL	ADAPL AND OR SPECIAL
A	

DISTRIBUTION STATEMENT A

Approved for public release
Distribution Unlimited

DDC
RECEIVED
MAY 25 1978
A


409359

Lee


A NONLINEAR UNIAXIAL INTEGRAL CONSTITUTIVE EQUATION INCORPORATING
RATE EFFECTS, CREEP, AND RELAXATION

E.P. Cernocky and E. Krempl
Department of Mechanical Engineering,
Aeronautical Engineering & Mechanics
Rensselaer Polytechnic Institute
Troy, New York 12181

ABSTRACT



A previously proposed first order nonlinear differential equation for uniaxial viscoplasticity, which is nonlinear in stress and strain but linear in stress and strain rates, is transformed into an equivalent integral equation. The proposed equation employs total strain only and is symmetric with respect to the origin and applies for tension and compression. The limiting behavior for large strains and large times for monotonic, creep, and relaxation loading is investigated and appropriate limits are obtained. When the equation is specialized to an overstress model it is qualitatively shown to reproduce key features of viscoplastic behavior. These include: initial linear elastic or linear viscoelastic response; immediate elastic slope for an instantaneous change in strain rate; normal strain rate sensitivity and nonlinear spacing of the stress-strain curves obtained at various strain rates; primary and secondary creep and relaxation such that the creep (relaxation) curves do not cross. Isochronous creep curves are also considered. Other specializations yield wavy stress-strain curves and inverse strain rate sensitivity. For cyclic loading the model must be modified to account for history dependence in the sense of plasticity.



Introduction

The subject of constitutive equations for metals is presently very active. Various approaches are being pursued which are intended to improve on the body of knowledge commonly referred to as plasticity. Although there are open questions regarding the foundation of plasticity in continuum mechanics theory the recent activity was mainly prompted by discrepancies between the observed metal deformation behavior and the predictions of plasticity theories.

A school of thought proposes new ideas in the framework of classical plasticity [1,2]; another group recognizes elastic and inelastic strains which are rate dependent [3]. Some motivate their approach by material science considerations [4-6]. Theories are also cast in terms of two sets of state variables evolving according to separately postulated growth laws. One set is responsible for rheological effects, the other for structural effects [7,8].

In the endochronic theories [9,10] a nondecreasing parameter is used in an integral or differential formulation and it has been shown that plasticity type phenomena can be reproduced without decomposition of the strain into elastic and plastic parts.

In previous publications [11,12] we have given operational definitions for aging, rate-dependence and history dependence in the sense of plasticity and have shown that not all postulated equations can reproduce what are commonly considered plasticity effects. We have further argued that plasticity effects are observed due to the internal changes in the material affected by the loading. Accordingly we postulated that a measure of internal change (separate from repositories for rate dependence and aging) should be introduced in a constitutive equation for metals. In [13] the properties of a continuously varying structure parameter together with an integral constitutive equation were investigated and it was shown that typical plasticity responses (cross-hardening,

cyclic hardening, Bauschinger effect) could be modelled. However, it was necessary to solve an integral equation to obtain the growth for the structure parameter.

A discontinuous growth law for the structure parameters was proposed in [11]. It was argued that in a continuum approach plasticity effects can only be recognized after unloading and reloading. According to this view plasticity and viscoplasticity are indistinguishable from nonlinear elasticity and nonlinear viscoelasticity, respectively as long as we consider only loading (see [11] footnote on p.75).

Here a previously proposed differential constitutive equation is represented as an equivalent integral equation. The integral formulation permits the study of the limiting behavior under large strains and large times. We demonstrate by qualitative arguments and by numerical experiments that the proposed "equation of state" can represent many key features of viscoplastic behavior as long as there is no substantial reversed loading involved. For reversed and cyclic loading the proposed nonlinear viscoelasticity law must be extended by the introduction of new origins and by updating the material parameters [11,14]. A three-dimensional formulation of the present theory is given separately.

The Proposed Constitutive Equation

For the uniaxial case we previously proposed [14,15]

$$m[\sigma, \epsilon] \dot{\epsilon} + g[\epsilon] = \sigma + k[\sigma, \epsilon] \dot{\sigma} \quad (1)$$

as the simplest constitutive equation capable of reproducing rate sensitivity, creep and relaxation. In the above, σ denotes the axial component of the Cauchy stress (true stress), ϵ is the engineering strain, and $\epsilon + 1$ is the axial component of the deformation gradient. The square brackets following a

symbol denote "function of" and the dot over a symbol denotes the material time derivative. Equation (1) is valid for infinitesimal and finite strain. The functions $m[]$ and $k[]$ are positive, bounded and are even functions for both variables taken together, i.e.

$$\text{and} \quad \left. \begin{aligned} m[\sigma, \epsilon] &= m[-\sigma, -\epsilon] \\ k[\sigma, \epsilon] &= k[-\sigma, -\epsilon] \end{aligned} \right\} \quad (2)$$

The function $g[]$ is odd. The functions $m[]$, $k[]$ and $g[]$ are assumed to have continuous derivatives.

The above stated requirements are derived from considering the qualitative behavior of materials in tension and compression and the responses predicted by (1). For the actual description of a particular material, the three material functions $m[]$, $k[]$, $g[]$ must be determined from experiments [16].

Integral Formulation

The constitutive equation (1) can be expressed as the following equivalent integral equations

$$\begin{aligned} \sigma[\tau] &= g[\epsilon[\tau]] + \int_0^t \left\{ \frac{m[\sigma[\tau], \epsilon[\tau]]}{k[\sigma[\tau], \epsilon[\tau]]} - g'[\epsilon[\tau]] \right\} \\ &\quad \exp\left(-\int_{\tau}^t \frac{dx}{k[\sigma[x], \epsilon[x]]}\right) \dot{\epsilon}[\tau] d\tau \end{aligned} \quad (3)$$

or

$$\epsilon[t] = \int_0^t \left\{ \frac{\dot{\sigma}[\tau] k[]}{m[]} + \frac{\sigma[\tau]}{m[]} \right\} \exp\left(-\int_{\tau}^t \frac{g[\epsilon[s]]}{\epsilon[s] m[\sigma[s], \epsilon[s]]} ds\right) d\tau \quad (4)$$

where we have assumed $\sigma(t=0) = 0$ and $\epsilon(t=0) = 0$. In the above, ' denotes the derivative of a function with regard to its argument^{*}.

^{*} In the case of discontinuous strain (stress) rates we propose (3) and (4) as fundamental forms.

It does not appear to be possible to represent (1) by an equation of the type

$$\sigma[\tau] = \int_0^t G[\epsilon[\tau], t-\tau] \dot{\epsilon}[\tau] d\tau \quad (5)$$

or

$$\epsilon[t] = \int_0^t J[\sigma[\tau], t-\tau] \dot{\sigma}[\tau] d\tau. \quad (6)$$

Equations (3) and (4) simplify to the regular convolution integrals of linear viscoelasticity if $g[\epsilon]$ is linear in ϵ and $m[\]$ and $k[\]$ are constants.

Behavior in Tensile Tests

We now use (3)[‡] to simulate a tensile test under constant strain rate $\dot{\epsilon} = \alpha$ such that

$$\epsilon = \alpha t. \quad (7)$$

We designate the response, i.e., the solution of (3) subject to (7) by

$$\hat{\sigma}[\epsilon] = \hat{\sigma}[\epsilon; \alpha] = \sigma[t] \big|_{\epsilon=\alpha t} \quad (8)$$

and α is considered a parameter.

Substitution of (7) into (3) using (8) yields

$$\hat{\sigma}[\epsilon; \alpha] = \hat{\sigma}[\epsilon] = g[\epsilon] + \int_0^\epsilon \left[\frac{m[\hat{\sigma}[x], x]}{k[\hat{\sigma}[x], x]} - g'[x] \right] \exp\left(-\frac{1}{\alpha} \int_x^\epsilon \frac{ds}{k[\hat{\sigma}[s], s]}\right) dx. \quad (9)$$

For extremely slow loading $\alpha \rightarrow 0$; we obtain from (9)

$$\hat{\sigma}[\epsilon; 0] = \lim_{\alpha \rightarrow 0} \hat{\sigma}[\epsilon; \alpha] = g[\epsilon] \quad (10)$$

and for extremely fast loading $\alpha \rightarrow \infty$, (9) furnishes

$$\hat{\sigma}[\epsilon; \infty] = \lim_{\alpha \rightarrow \infty} \hat{\sigma}[\epsilon; \alpha] = \int_0^\epsilon \frac{m[\hat{\sigma}[x], x]}{k[\hat{\sigma}[x], x]} dx. \quad (11)$$

[‡] Appendix I shows the parallel development for (4)

From (10) we see that $g[\epsilon]$ furnishes the stress-strain curve which is obtained for extremely slow loading. We designate the stress-strain relationship for infinitely fast loading by $g^*[\epsilon]$. From (11) we have for infinitely fast loading

$$\frac{m[\hat{\sigma}[\epsilon], [\epsilon]]}{k[\hat{\sigma}[\epsilon], [\epsilon]]} = g'^*[\epsilon]. \quad (12)$$

The relation (12) between $m[]$ and $k[]$ is only required for fast loading. However, as a useful and physically motivated simplification of the theory, we propose (12) to be true for all loadings. Consequently (9) is rewritten as

$$\hat{\sigma}[\epsilon; \alpha] = \hat{\sigma}[\epsilon] = g[\epsilon] + \int_0^\epsilon \left\{ g'^*[x] - g'[x] \right\} \exp\left(-\frac{1}{\alpha} \int_x^\epsilon \frac{ds}{k[\hat{\sigma}[s], s]}\right) dx. \quad (13)$$

Using (12) we can also rewrite (1), (3) and (4) accordingly.

From (13) we see immediately that for every $\epsilon \geq 0$ and $\alpha \geq 0$,

$$g^*[\epsilon] \geq \hat{\sigma}[\epsilon; \alpha] \geq g[\epsilon] \quad (14)$$

provided $g'^*[\epsilon] - g'[\epsilon] \geq 0$. Therefore, the response for $0 \leq \alpha \leq \infty$ is between the extremely fast and the extremely slow response. Moreover for $\alpha_2 > \alpha_1 > 0$ we have for every positive ϵ

$$\hat{\sigma}[\epsilon; \alpha_2] \geq \hat{\sigma}[\epsilon; \alpha_1] \quad (15)$$

so that the stress-strain curve for the fast rate is above the curve for the slow rate, as shown in Fig.1. The above behavior reflected in the relations (14) and (15) would be reversed by setting $g'^*[\epsilon] - g'[\epsilon] \leq 0$ for $\epsilon \geq 0$.

For $\alpha \leq 0$ the responses are symmetric with respect to the origin by virtue of (2) and the fact that g is odd.

Differentiation of (13) with respect to ϵ yields

$$\frac{d\hat{\sigma}}{d\epsilon} = g'^*[\epsilon] - \frac{1}{\alpha k[\hat{\sigma}[\epsilon], \epsilon]} \int_0^\epsilon \left\{ g'^*[x] - g'[x] \right\} \exp\left(-\frac{1}{\alpha} \int_x^\epsilon \frac{ds}{k[\hat{\sigma}[s], s]}\right) dx. \quad (16)$$

Performing the limits for $\alpha \rightarrow 0$ and $\alpha \rightarrow \infty$ in (16) we obtain results consistent with (10) and (11), (12), respectively. Moreover we see that

$$\frac{d\hat{\sigma}}{d\epsilon} [\epsilon = 0] = g'^* [0] \quad (17)$$

for all α . All the curves in Fig.1 have therefore one initial common slope equal to the initial slope of g^* irrespective of the loading rate.

Behavior at Large Strains

We are interested in the behavior of our model at large strains in a tensile test. To this end we investigate (16) for the mathematical idealization $\epsilon \rightarrow \infty$ for $\alpha = \text{const.}^\dagger$. The resulting indeterminate expression is resolved (see Appendix II) to obtain

$$\lim_{\epsilon \rightarrow \infty} \frac{d\hat{\sigma}}{d\epsilon} = g'[\infty] \quad (18)$$

for all finite α and provided $g'[\infty]$, $g'^*[\infty]$ and $k[\infty, \infty]$ exist and are finite^{##}. This is a very strong result requiring that all response curves become parallel to each other for large strains. Figure 2, which represents the results of the numerical integration of (13), demonstrates this behavior. For convenience k was selected to be constant. Initially linear elastic behavior is obtained as $g'[0] = g'^*[0]$. The representation of the g and g^* functions follows the development of the $y(x)$ functions using the second kernel of [22].

[†] While these mathematical limits may seem unrealistic they are indeed useful because the solutions of the equations are rapidly asymptotic to these limits; see Fig.2.

^{##} Throughout this paper we consider only k -functions which are bounded. In the case where $k[\sigma, \epsilon] = k[\sigma - f(\epsilon)]$ for some function f , we similarly require that $k[\infty]$ be finite.

Performing the limit for (13) in a similar manner we obtain

$$\lim_{\epsilon \rightarrow \infty} (\hat{\sigma} - g[\epsilon]) = (g'[\infty] - g'[\infty]) \alpha k[\hat{\sigma}[\infty], \infty]. \quad (19)$$

The limiting value of $(\hat{\sigma} - g[\epsilon])$ is finite and is determined by the strain rate and the values of the functions $k[\]$, $g'[\]$, $g'^*[\]$ at infinity.

The relations (18) and (19) were derived for constant strain rate loading. By starting with (3) and investigating the limit for $t \rightarrow \infty$ the following expressions result:

$$\lim_{t \rightarrow \infty} \dot{\sigma}[t] = g'[\epsilon[\infty]] \dot{\epsilon}[\infty] \quad (20)$$

and

$$\lim_{t \rightarrow \infty} (\sigma - g[\epsilon[t]]) = (g'^*[\epsilon[\infty]] - g'[\epsilon[\infty]]) \dot{\epsilon}[\infty] k[\sigma[\infty], \epsilon[\infty]] \quad (21)$$

provided $\dot{\epsilon}[\infty]$ together with the limits of the other functions exist and are finite.

If $\epsilon[\infty] = \infty$ the expressions (20) and (21) are identical to (18) and (19), respectively, the only exception being that $\hat{\sigma}[\epsilon]$, the response to constant strain rate forcing, appears in (18) and (19) whereas the response in (20) and (21) is $\sigma[t]$. Therefore the responses for large strain and time under variable $\dot{\epsilon}$ become identical to the ones under constant $\dot{\epsilon} = \alpha$ provided $\dot{\epsilon}[\infty] = \alpha$ and it is not necessary to have always constant strain rate on $0 \leq t \leq \infty$ to arrive at $\lim_{t \rightarrow \infty} \frac{d\sigma}{d\epsilon} = g'[\epsilon[\infty]]$.

Instantaneous Change of Strain Rate

We consider two tensile tests with respective strain rates α_2 and α_1 with $\alpha_2 > \alpha_1 > 0$. Then from previous arguments we know that $\hat{\sigma}[\epsilon, \alpha_2] \geq \hat{\sigma}[\epsilon, \alpha_1]$. Suppose instead that we initially load with α_1 and at some time t_0 and associated strain ϵ_0 we instantaneously change the strain rate from α_1 to α_2 as shown in Fig.3. We call $\hat{\sigma}_A[\epsilon]$ the response to α_2 and $\hat{\sigma}_B[\epsilon]$ the response to α_1 followed by α_2 as shown in Fig.3.

First we investigate the $\hat{\sigma}$ vs. ϵ relationship. For $\epsilon \leq \epsilon_0$, $\hat{\sigma}_A[\epsilon] \geq \hat{\sigma}_B[\epsilon]$ by previous arguments. For $\epsilon \geq \epsilon_0$ the respective responses are

$$\hat{\sigma}_A[\epsilon] = g[\epsilon] + \int_0^\epsilon (g'^*[x] - g'[x]) \exp\left(-\frac{1}{\alpha_2} \int_x^\epsilon \frac{ds}{k[\hat{\sigma}_A[s], s]}\right) dx \quad (22)$$

and

$$\begin{aligned} \hat{\sigma}_B[\epsilon] = g[\epsilon] + \int_{\epsilon_0}^\epsilon (g'^*[x] - g'[x]) \exp\left(-\frac{1}{\alpha_2} \int_x^\epsilon \frac{ds}{k[\hat{\sigma}_B[s], s]}\right) dx \\ + (\hat{\sigma}_B[\epsilon_0] - g[\epsilon_0]) \exp\left(-\frac{1}{\alpha_2} \int_{\epsilon_0}^\epsilon \frac{ds}{k[\hat{\sigma}_B[s], s]}\right). \end{aligned} \quad (23)$$

where for $\epsilon \geq \epsilon_0$, $\hat{\sigma}_B[\epsilon] = \hat{\sigma}_B[\alpha_2 t - (\alpha_2 - \alpha_1)t_0] = \sigma[t]$.

For large strains ($\epsilon \rightarrow \infty$) we obtain from (22)

$$\lim_{\epsilon \rightarrow \infty} (\hat{\sigma}_A - g[\epsilon]) = \{g'^*[\infty] - g'[\infty]\} \alpha_2 k[\hat{\sigma}_A[\infty], \infty] \quad (24)$$

and from (23)

$$\lim_{\epsilon \rightarrow \infty} (\hat{\sigma}_B - g[\epsilon]) = \{g'^*[\infty] - g'[\infty]\} \alpha_2 k[\hat{\sigma}_B[\infty], \infty]. \quad (25)$$

Unless $k[\hat{\sigma}_A[\infty], \infty] = k[\hat{\sigma}_B[\infty], \infty]$ the two paths on the $\hat{\sigma}$ - ϵ plane will not coincide for large values of strain. In both cases the slopes approach $g'[\infty]$ as $\epsilon \rightarrow \infty$. We see therefore that the two curves, i.e., $\hat{\sigma}_A$ and $\hat{\sigma}_B$, become parallel at large strains.

The question arises whether the path $\hat{\sigma}_A$ can be crossed by path $\hat{\sigma}_B$. From (1), (12) and the chain rule we obtain

$$\frac{d\hat{\sigma}}{d\epsilon} = g'^*[\epsilon] - \frac{\hat{\sigma} - g[\epsilon]}{k[\hat{\sigma}[\epsilon], \epsilon] \alpha}. \quad (26)$$

From Eq. (26) we see that for a given stress, strain, and strain rate, there exists a unique slope $\frac{d\hat{\sigma}}{d\epsilon}$ irrespective of the prior history. Since crossing of the $\hat{\sigma}_A$ and $\hat{\sigma}_B$ curves would require a nonunique slope at the crossing

point, the condition necessary for crossing cannot be met and $\hat{\sigma}_A \geq \hat{\sigma}_B$ always; the two curves can never cross^{*}.

To investigate the behavior at large times we start from (3) and obtain (note σ_A and σ_B are the responses in σ -time coordinates)

$$\lim_{t \rightarrow \infty} (\sigma_A - g[\alpha_2 t]) = (g'[\infty] - g'[\infty])\alpha_2 k[\sigma_A[\infty], \infty] \quad (27)$$

and

$$\lim_{t \rightarrow \infty} (\sigma_B - g[\alpha_1 t_0 + \alpha_2 (t - t_0)]) = (g'[\infty] - g'[\infty])\alpha_2 k[\sigma_B[\infty], \infty]. \quad (28)$$

If $g'[\infty] = E_S$ then we have

$$\lim_{t \rightarrow \infty} (\sigma_A - \sigma_B + E_S t_0 (\alpha_2 - \alpha_1)) = (g'[\infty] - E_S)\alpha_2 (k[\sigma_A[\infty], \infty] - k[\sigma_B[\infty], \infty]). \quad (29)$$

Even if the right-hand side of (29) would be zero, $\sigma_A[\infty] - \sigma_B[\infty] \neq 0$, i.e., the graphs of σ_A vs. time and σ_B vs. time do not coincide. The corresponding $\hat{\sigma}$ - ϵ graphs, however, may eventually coincide as can be seen from (24) and (25).

So far we have only considered $\alpha_2 > \alpha_1 > 0$. The previous arguments can be extended to the case of $\alpha_1 > \alpha_2 > 0$ with the result that the curve for $\hat{\sigma}_B$ vs. ϵ will approach $\hat{\sigma}_A$ vs. ϵ from above but will never cross the $\hat{\sigma}_A$ curve.

Change of Slope

The slopes at point A in Fig.3 approached from the left and from the right are determined from (16) or (26) to be

$$\lim_{\epsilon \rightarrow \epsilon_0^-} \frac{d\hat{\sigma}_B}{d\epsilon} = g'[\epsilon_0] - \frac{\hat{\sigma}_B[\epsilon_0] - g[\epsilon_0]}{\alpha_1 k[\hat{\sigma}_B[\epsilon_0], \epsilon_0]} \quad (30)$$

and

$$\lim_{\epsilon \rightarrow \epsilon_0^+} \frac{d\hat{\sigma}_B}{d\epsilon} = g'[\epsilon_0] - \frac{\hat{\sigma}_B[\epsilon_0] - g[\epsilon_0]}{\alpha_2 k[\hat{\sigma}_B[\epsilon_0], \epsilon_0]} \quad (31)$$

^{*} This argument is due to Dr. H. Moon.

so that the slopes differ by

$$\Delta \equiv \frac{d\hat{\sigma}_B}{d\epsilon} (\epsilon = \epsilon_o^+) - \frac{d\hat{\sigma}_B}{d\epsilon} (\epsilon = \epsilon_o^-) = \frac{\alpha_2 - \alpha_1}{\alpha_2 \alpha_1} \cdot \frac{\hat{\sigma}_B[\epsilon_o] - g[\epsilon_o]}{k[\hat{\sigma}_B[\epsilon_o], \epsilon_o]} \quad (32)$$

We obtain therefore an instantaneous change in the slope of the $\sigma - \epsilon$ curve as the strain rate is changed instantaneously from α_1 to α_2 . For $\alpha_2 > \alpha_1$ the right-hand side of (32) is positive so that $\frac{d\sigma_B}{d\epsilon} (\epsilon = \epsilon_o^+) > \frac{d\sigma_B}{d\epsilon} (\epsilon = \epsilon_o^-)$. For $\alpha_1 > \alpha_2 > 0$ the opposite is true.

Behavior at Small Stresses (Strains)

Here we are interested in the behavior around the origin. Suppose that for $|\epsilon| \leq \epsilon_a$ ($\epsilon_a > 0$) the functions g and g^* can be approximated by $g[\epsilon] = E\epsilon$ (E is Young's Modulus) and $g^*[\epsilon] = E^*\epsilon$ and that $m[\]$ and $k[\]$ are constant for all $|\epsilon| \leq \epsilon_a$ and associated $|\sigma| \leq \sigma_a$ ($\sigma_a > 0$) and equal to m_a and k_a , respectively. Then from (3) for $|\epsilon| \leq \epsilon_a$

$$\sigma[t] = E\epsilon + \int_0^t (E^* - E) \exp\left(-\frac{1}{k_a} (t - \tau)\right) \dot{\epsilon} d\tau \quad (33)$$

For $E^* > E$ (33) is the standard linear solid of viscoelasticity. For $E^* = E$ initial linear elastic behavior is reproduced on $|\epsilon| \leq \epsilon_a$, even for nonconstant m and k . These two models are important representations of solids and can be easily obtained from (1) just by constructing the coefficient functions appropriately [22].

Creep and Relaxation

We use Eq. (3) to compute the stress response in a relaxation test where the strain is increased to some value ϵ_o and then kept constant such that $\dot{\epsilon} = 0$. We assume the strain history to be given by

$$\begin{aligned}\dot{\epsilon} &= \dot{\epsilon}[t] & 0 \leq t < t_0 & \text{ with } \epsilon[t_0] = \epsilon_0 \\ \dot{\epsilon} &= 0 & t \geq t_0\end{aligned}$$

where $\dot{\epsilon}[t]$ is some smooth function of time. From (3), using (12), we obtain for the relaxation stress σ_R for $t \geq t_0$

$$\begin{aligned}\sigma_R[t] &= g[\epsilon_0] + \left(\exp - \int_{t_0}^t \frac{dx}{k[\sigma_R[x], \epsilon_0]} \right) (\sigma_R[\epsilon_0] - g[\epsilon_0]) \\ \text{where} \\ \sigma_R[\epsilon_0] - g[\epsilon_0] &= \int_0^{\tau} \{g'[\epsilon(\tau)] - g'[\epsilon_0]\} \exp \left\{ \int_{t_0}^{\tau} \frac{dx}{k[\sigma_R[x], \epsilon[x]]} \right\} \dot{\epsilon}(\tau) d\tau.\end{aligned}\quad (34)$$

Alternatively if $\epsilon[t] = \epsilon_0 h[t - t_0]$ and $\dot{\epsilon}[t] = \epsilon_0 \delta[t - t_0]$ where $h[t]$ and $\delta[t]$ are the step function and the Delta function, respectively, i.e., if we consider an instantaneous loading from zero to ϵ_0 at time t_0 we obtain from (3), for $t \geq t_0$, respectively,

$$\sigma_\delta[t] = g[\epsilon_0] + \{g^*[\epsilon_0] - g[\epsilon_0]\} \exp - \int_{t_0}^t \frac{dx}{k[\sigma_\delta[x], \epsilon_0]} \quad (35)$$

where $\sigma_\delta[t]$ is the relaxation stress due to the impulsive strain input.

Differentiation of (34) and (35) shows that the relaxation rate is always negative or zero provided $g^* - g' \geq 0$. For large times $t \rightarrow \infty$, $\sigma[t \rightarrow \infty] = g[\epsilon_0]$ for both (34) and (35). The curve $g[\epsilon]$ is therefore not only the slow loading curve but also the terminal curve of all relaxation tests.

From (35) we see that the impulsive stress relaxation starts at $t = t_0$ from $g^*[\epsilon_0]$, i.e., from the curve traced out in the infinitely fast constant strain rate loading. If the loading up to ϵ_0 is smooth, such as by constant strain rate, then we observe from (34) that the relaxation starts from a point on the curve traced out in the constant strain rate test.

The decrease in stress during the relaxation test is controlled by the function $k[\cdot]$. We may therefore call it the relaxation function. To demonstrate the effect of the function k on relaxation behavior we have computed the relaxation from a point on g^* in Fig.4. Curve 1 corresponds to constant k and (34), (35) are linear in stress. For curve 2 $k = k[\sigma - g[\epsilon]]$ as in Fig.10 so that (34) and (35) are nonlinear in stress. In Fig.4 the time scale depends upon the time scale used for k ; if k is given in units of hours then the abscissa is measured in terms of hours.

Appendix III gives a discussion of the creep equation obtained from (4). A comparison of (34) with the corresponding creep equation (All) shows that the exponential decay in a creep test is controlled by $m[\cdot]$, $g[\cdot]$ and $\epsilon[\cdot]$ and involves a complicated interaction of these quantities. Although creep and relaxation show an exponential type of decay, their detailed evolution is quite different.

Spacing of Creep and Relaxation Curves

Consider a series of creep (relaxation) tests performed at an increasing sequence of constant stress (strain) values; we require that the resulting curves of strain vs. time (stress vs. time) and of strain rate vs. time (stress rate vs. time) are nonintersecting as is usually the case with actual test results. Further we require that any two curves $\epsilon_2[t]$ and $\epsilon_1[t]$, ($\sigma_2[t]$ and $\sigma_1[t]$) associated with two constant stresses $\sigma_o^2 > \sigma_o^1$ (constant strains $\epsilon_o^2 > \epsilon_o^1$) satisfy the condition $\epsilon_2[t] \geq \epsilon_1[t]$ for any time t ($\sigma_2[t] \geq \sigma_1[t]$) and that $\dot{\epsilon}_2[t] \geq \dot{\epsilon}_1[t]$ ($\dot{\sigma}_2[t] \geq \dot{\sigma}_1[t]$). These conditions require that

$$\frac{\partial \epsilon[t]}{\partial \sigma_o} \geq 0 \text{ and } \frac{\partial \dot{\epsilon}[t]}{\partial \sigma_o} \geq 0 \quad (36)$$

and

$$\frac{\partial \sigma[t]}{\partial \epsilon_0} \geq 0 \text{ and } \frac{\partial \dot{\sigma}[t]}{\partial \epsilon_0} \geq 0 \quad (37)$$

for the creep and relaxation test, respectively; $\epsilon[t]$, $\dot{\epsilon}[t]$ in (36) depend parametrically upon σ_0 , and $\sigma[t]$, $\dot{\sigma}[t]$ in (37) depend parametrically upon ϵ_0 .

If we specialize (1) for the creep test ($\dot{\sigma} = 0$, $\sigma = \sigma_0$) and perform the differentiation, with respect to σ_0 , we obtain

$$\frac{\partial \dot{\epsilon}[t]}{\partial \sigma_0} = \frac{F[t] - \frac{\partial \epsilon[t]}{\partial \sigma_0} H[t]}{m[\sigma_0, \epsilon[t]]^2} \quad (38)$$

where

$$F[t] = m[\sigma_0, \epsilon[t]] - (\sigma_0 - g[\epsilon[t]]) \frac{\partial m[\sigma_0, \epsilon[t]]}{\partial \sigma_0} \quad (39)$$

and

$$H[t] = m[\sigma_0, \epsilon[t]] g'[\epsilon[t]] + (\sigma_0 - g[\epsilon[t]]) \frac{\partial m[\sigma_0, \epsilon[t]]}{\partial \epsilon} \quad (40)$$

Equation (38) is integrated to obtain

$$\begin{aligned} \frac{\partial \epsilon[t]}{\partial \sigma_0} = & \int_0^t \frac{F[\tau]}{m[\sigma_0, \epsilon[\tau]]^2} \left(\exp - \int_{\tau}^t \frac{H[x]}{m[\sigma_0, \epsilon[x]]^2} dx \right) d\tau \\ & + \frac{\partial \epsilon[0]}{\partial \sigma_0} \exp - \int_0^t \frac{H[x]}{m[\sigma_0, \epsilon[x]]^2} dx \end{aligned} \quad (41)$$

where in (41) $t=0$ corresponds to the initiation of creep, $\epsilon[0] \neq 0$.

When $\frac{\partial \epsilon[t=0]}{\partial \sigma_0} \geq 0$ from (38) and (39) we see that sufficient conditions for satisfying (36) are

$$F[t] \geq 0 \text{ and } F[t] - \frac{\partial \epsilon[t]}{\partial \sigma_0} H[t] \geq 0. \quad (42)$$

Following similar procedures for relaxation, sufficient conditions for satisfying (37) are, respectively

$$P[t] = k[\sigma[t], \epsilon_0] g'[\epsilon_0] + (\sigma[t] - g[\epsilon_0]) \frac{\partial k[\sigma[t], \epsilon_0]}{\partial \epsilon_0} \geq 0 \quad (43)$$

and

$$P[t] - \frac{\partial \sigma[t]}{\partial \epsilon_0} Q[t] \geq 0 \quad (44)$$

with

$$Q[t] = k[\sigma[t], \epsilon_0] - (\sigma[t] - g[\epsilon_0]) \frac{\partial k[\sigma[t], \epsilon_0]}{\partial \sigma} \quad (45)$$

The examination of (39) - (42) shows that the no crossing conditions (36) and (37) are in general not satisfied.

From Eqs. (38) - (41) and their counterparts for relaxation, we obtain the limits for large times

$$\lim_{t \rightarrow \infty} \frac{\partial \epsilon[t]}{\partial \sigma_0} = \lim_{t \rightarrow \infty} \left(\frac{F[t]}{H[t]} \right) = \frac{1}{g'[\epsilon[\infty]]} \quad (46)$$

$$\lim_{t \rightarrow \infty} \frac{\partial \dot{\epsilon}[t]}{\partial \sigma_0} = 0 \quad (47)$$

$$\lim_{t \rightarrow \infty} \frac{\partial \sigma[t]}{\partial \epsilon_0} = \lim_{t \rightarrow \infty} \left(\frac{P[t]}{Q[t]} \right) = g'[\epsilon[\infty]] \quad (48)$$

$$\lim_{t \rightarrow \infty} \frac{\partial \dot{\sigma}[t]}{\partial \epsilon_0} = 0. \quad (49)$$

where we have assumed that in creep or relaxation $(\sigma - g) \rightarrow 0$ as $t \rightarrow \infty$. Therefore (46) and (47) do not hold for those creep conditions for which there is no solution to the equation

$$\sigma_0 = g[\epsilon] \quad (50)$$

i.e., in those cases for which (1) reproduces secondary or tertiary creep; see also Appendix III.

Useful Specializations of (1)

- A) The Functions $m[]$ and $k[]$ are Selected to Depend Upon $(\sigma - g[\epsilon])$
and $g'[\epsilon] = E$ (Modulus of Elasticity)[‡]

Because of this special dependence σ and ϵ have no independent influence on the behavior of (1). For a given loading rate the properties of (1) are determined by the value of $\sigma - g[\epsilon]$ alone, and curves equidistant to $\sigma = g[\epsilon]$ are curves along which the properties of solutions of (1) are identical.

Specifically with reference to (26) we see that the slope $\frac{d\hat{\sigma}}{d\epsilon}$ for a given constant $\dot{\epsilon}$ is constant on a curve $\sigma - g[\epsilon] = \text{const.}$ Moreover for $\sigma - g[\epsilon] = 0$ $\frac{d\hat{\sigma}}{d\epsilon} = E$ irrespective of the strain rate. The slopes of all of the curves departing from the curve $\sigma = g[\epsilon]$ are all equal to the elastic modulus. (It is however, not possible to depart from $\sigma - g[\epsilon] = 0$ by creep or relaxation, as can be easily verified from (1).) With the $\sigma - g[\epsilon]$ dependence in the functions the curve $\sigma = g[\epsilon]$ assumes special significance since along it the behavior predicted by (1) is the same as at the origin.

While every solution curve of (1) for constant or variable strain rate must become parallel to $g[\epsilon]$ [see (18) and (20)] only the $\sigma - g[\epsilon]$ dependence in k models a nonlinear dependence between α and $\hat{\sigma} - g[\epsilon]$. Consider now two tests with α_1 and α_2 and associated stress responses $\hat{\sigma}_1$ and $\hat{\sigma}_2$, respectively. From (19) we obtain the ratio

$$\frac{(\hat{\sigma}_1[\infty] - g[\infty])k[\hat{\sigma}_2[\infty] - g[\infty]]}{(\hat{\sigma}_2[\infty] - g[\infty])k[\hat{\sigma}_1[\infty] - g[\infty]]} = \frac{\alpha_1}{\alpha_2} \quad (51)$$

and therefore $(\hat{\sigma}_1 - g[\infty])$ and $(\hat{\sigma}_2 - g[\infty])$ are related in a nonlinear fashion. For any other choice of the σ , ϵ dependence in the functions $m[]$ and $k[]$

‡

We recall the conditions $k(\infty) = \text{finite}$ and k positive.

we have for $\hat{\sigma}_1[\infty] = \hat{\sigma}_2[\infty] = \infty$, $k[\hat{\sigma}_1[\infty], \infty] = k[\hat{\sigma}_2[\infty], \infty]$ ^{*} so that the ratio (51) reduces to

$$\frac{\hat{\sigma}_1[\infty] - g[\infty]}{\hat{\sigma}_2[\infty] - g[\infty]} = \frac{\alpha_1}{\alpha_2} \quad (52)$$

Only the $\hat{\sigma} - g[\epsilon]$ dependence in k , therefore, yields a nonlinear relation between the differences $\hat{\sigma} - g[\epsilon]$ at large strain in tensile tests with various strain rates. Such nonlinear relations are usually observed in real tensile tests. Figures 7a, 7b, 9 and 10 illustrate this property.

The limits (51) and (18) are valid only at $\epsilon \rightarrow \infty$. However, the stress ratio and the stress slope are rapidly asymptotic to these limiting values [(51) and (18)], as shown in Figs. 2, 5 through 10. Moreover, the $(\sigma - g[\epsilon])$ -dependence appears to enhance the rate with which these limits are obtained.

From (24) and (25) we obtain in the case of an instantaneous change of strain rate

$$\frac{\hat{\sigma}_A[\infty] - g[\infty]}{k[\hat{\sigma}_A[\infty] - g[\infty]]} = (E - g'[\infty])\alpha_2 \quad (53)$$

and

$$\frac{\hat{\sigma}_B[\infty] - g[\infty]}{k[\hat{\sigma}_B[\infty] - g[\infty]]} = (E - g'[\infty])\alpha_2 \quad (54)$$

From our previous restrictions upon the function k we have $\hat{\sigma}_A = \hat{\sigma}_B$ in this case.

Aside from insuring that $\frac{d\hat{\sigma}}{d\epsilon} = E$ for $\hat{\sigma} - g[\epsilon] = 0$, setting $g'^*[\epsilon] = E$ has the following consequences for the test involving a change in the strain rate, see Fig. 3. Suppose the function $g[\epsilon]$ has the shape of a stress-strain diagram as shown in Fig. 1, then we know from (16) and (18) that $\frac{d\hat{\sigma}}{d\epsilon}$ approaches $g'[\epsilon]$ in a constant strain (stress) rate test. If $\frac{d\hat{\sigma}_B}{d\epsilon} \approx g'[\epsilon]$ and $g'[\epsilon] \ll E$ then

* If $\hat{\sigma}_1[\infty]$ and $\hat{\sigma}_2[\infty]$ are finite then $k[\hat{\sigma}_1[\infty], \infty]$ may not be equal to $k[\hat{\sigma}_2[\infty], \infty]$. This may occur if $g'[\infty] = 0$.

the second term on the right-hand side of (30) is close to the value E . If the strain rate is now increased instantaneously by one or several orders of magnitude then the slope $\frac{d\hat{\sigma}}{d\epsilon} \frac{B}{(\epsilon - \epsilon_0^+)}$ in (31) will be approximately equal to E since the second term in (31) becomes negligible. Therefore the instantaneous change in slope predicted by (1) is approximately the elastic slope E . The above specialization insures that this behavior is independent of strain.

B) The Derivatives $m' = \frac{d[\sigma - g[\epsilon]]}{d(\sigma - g[\epsilon])} < 0$ and $k' < 0$

This specialization provides a sufficient condition for

$$\frac{d\hat{\sigma}}{d\epsilon} \geq g'[\epsilon] \text{ in a tensile loading provided } \epsilon > 0, E = g'^*[\epsilon] \geq g'[\epsilon] \text{ and } \dot{\epsilon} = \alpha$$

$$\ddot{\epsilon}[t] \leq 0 \text{ in a creep test provided } g'[\epsilon] \geq 0$$

$$\ddot{\sigma}[t] \geq 0 \text{ in a relaxation test}$$

$$\frac{\partial \epsilon[t]}{\partial \sigma_0} \geq 0 \text{ in (41), the creep curves do not cross, i.e.,}$$

$$\epsilon[t]_{\sigma_1} \geq \epsilon[t]_{\sigma_2} \text{ for } \sigma_1 > \sigma_2 > 0 \text{ and every } t.$$

$$\frac{\partial \sigma[t]}{\partial \epsilon_0} \geq 0 \text{ the relaxation curves do not cross and } \sigma[t]_{\epsilon_1} \geq \sigma[t]_{\epsilon_2} \text{ for } \epsilon_1 \geq \epsilon_2.$$

Further the no crossing conditions for the creep rate curves $\left(\frac{\partial \dot{\epsilon}[t]}{\partial \sigma_0} \geq 0\right)$ and for the relaxation rate curves $\left(\frac{\partial \dot{\sigma}[t]}{\partial \epsilon_0} \geq 0\right)$ appear to be satisfied.

It can be demonstrated that for k either constant or depending upon $\sigma - g[\epsilon]$ with $\frac{dk(\sigma - g[\epsilon])}{d(\sigma - g[\epsilon])} = k' \leq 0$ and $g'^*[\epsilon] = E$, $\frac{d\hat{\sigma}}{d\epsilon} \geq g'[\epsilon]$ provided $\dot{\epsilon} = \alpha > 0$, as shown in Figs. 2, 7a, 7b and 10. However, if the difference $g'^* - g'$ is not always positive or if g'^* is nonlinear, then wavy stress-strain curves may result as shown in Fig. 5. In proceeding from Fig. 2 to Fig. 5 only g'^* was altered from a linear to a nonlinear relation. Further examples of causes of waviness are given in Figs. 6 and 8. If k is neither constant nor dependent on $\sigma - g[\epsilon]$ wavy stress-strain curves may also occur even if g'^* is constant as shown in

Fig.9. Note that waviness disappears when k is made to depend on $\sigma - g[\epsilon]$ as was done in Fig.10.

Waviness of the stress-strain curves can also be obtained by making the equilibrium curve g "wavy" as demonstrated in Figs.7a and 7b. In both cases $\dot{g} = E\dot{\epsilon}$. The g -curve is constructed in such a way as to resemble the yielding of carbon steel. In Fig.7a $k = 3.2$ s. The k -function of Fig.7b taken from [16] depends on $\sigma - g[\epsilon]$ and the $\hat{\sigma}$ -curves for various strain rates follow the $g[\epsilon]$ -curve until the dip disappears at $\alpha = 10^{-1} \text{ s}^{-1}$. Owing to the constant value of k only the $\hat{\sigma}$ -curve for $\alpha = 10^{-4} \text{ s}^{-1}$ follows $g[\epsilon]$ in Fig.7a. The curves for the higher strain rates are coincident with $\dot{g} = E\dot{\epsilon}$. They will become parallel to $g[\epsilon]$ at $\hat{\sigma} - g[\epsilon]$ values determined by (19). These values are beyond the limits of Fig.7a.

A comparison of Figs.7a and 7b shows the importance of the $\sigma - g[\epsilon]$ -dependence in k to provide for an early "locking in" and for the nonlinear spacing of the $\hat{\sigma}$ -curves obtained at various α , see Eq. (51).

Discussion

The model (1) subject to specializations A) and B) reproduces in a unified way many of the characteristic features of metal deformation behavior generally referred to as isothermal dynamic plasticity or viscoplasticity. These include

- Uniform slope at the origin
- Linear elastic or linear viscoelastic behavior at small strain (stress)
- Initial elastic response upon a jump in strain rate
- Nonlinear spacing of the stress-strain curves at various strain rates
- Elastic response for very fast loading
- Existence of an equilibrium stress-strain curve
- Creep and relaxation.

In addition to the qualitative arguments discussed herein we demonstrate in [16] by numerical experiments which simulate constant rate loadings with various stress (strain) rates, with tension-tension cycling, and creep and relaxation conditions that the general appearance of the numerically obtained responses is very reminiscent of the actual behavior of metals. We therefore see that a nonlinear viscoelastic constitutive equation such as (1) subject to the specializations A) and B) can reproduce viscoplasticity very well. However, the correspondence ceases to hold if $\sigma - g[\epsilon]$ would change sign. At this point modifications will be necessary such as discussed in [11]. A forthcoming paper will address this subject.

Making the functions depend upon $\sigma - g[\epsilon]$ renders (1) in essence an overstress model [17,18] which has been considered many times [19]. However, the previous use of the overstress concept is either tied to the usual decomposition of the strains into elastic and plastic parts and the yield surface concept [18,19] or to very specific functions [17]. Here we have demonstrated that none of these concepts are necessary to reproduce metal behavior qualitatively as long as there is no substantial unloading involved. Moreover creep and relaxation are included in (1) in a unified way. Also we have explored and shown the limits obtained from (1) for various extreme conditions which to the authors' knowledge has not been done before.

We note that isochronous creep curves which are a common way of representing creep data in engineering [20,21] can be obtained from (1). Isochronous creep curves are σ_0 vs. ϵ cross-plots (where σ_0 is a parameter) of regular creep curves for constant creep time.

Considering (41) and the derivation of it we see that it represents for $t = \text{constant}$ the reciprocal of the slope of the isochronous creep curve. Condition (42) ensures that $\frac{\partial \epsilon[t]}{\partial \sigma_0} \geq 0$; i.e., the slope of the isochronous creep curve will be positive. Isochronous creep curves of metals [20] and plastics [21] have this property.

In the interpretation of the limit obtained in (46) the condition $t \rightarrow \infty$ refers physically to a long-time creep curve. The limit (46) indicates that the slope of this infinitely large time isochronous creep curve is

$$\frac{d\sigma_0}{d\epsilon} = g'[\epsilon[t = \infty]] \quad (55)$$

from which we infer that it must be equal to the slope of the equilibrium stress-strain curve. This inference is only valid if the stress σ_0 is such that $\epsilon(t = \infty) = g^{-1}[\sigma_0]$; see Eq. (50) and Appendix III.

These reflections suggest then that $g[\epsilon]$ could be obtained from a long term isochronous creep curve, say for $t = 300,000$ hours for the case of metals, and could be obtained from [20].

In the above we have concentrated on the specializations A) and B) which appear to be appropriate for metals. However, other properties of (1) resulting from different specializations are of interest for the modelling of other materials.

If g and g^* are selected such that $g^* - g' < 0$ then inverse strain rate sensitivity results such as that shown in Fig.6 which is obtained from Fig.5 by interchanging g^* and g . It can be seen that the "slow" stress-strain curves are above the fast ones, reversing the trend of Fig.5 and the relation (15).

It is also possible to have "classical" strain rate sensitivity over one strain interval and "reverse" strain rate sensitivity over another interval by making g and g^* intersect once. The resulting stress-strain curves are shown in Fig.8.

In Figs.2, 5 - 7 the initial slopes of g^* and g are made equal. In these cases all the curves are initially coincident and we have initial linear elastic behavior. In Fig.8, $g'^* > g'$ initially (k is constant in this example), and therefore a linear viscoelastic behavior results.

Figure 8 also illustrates that all curves with nonvanishing strain rate have initially the same slope as stated in (17).

If we begin a creep ($\dot{\sigma} = 0$) or a relaxation ($\dot{\epsilon} = 0$) test on any stress-strain curve then strain (stress) would always move towards g . Specifically in Fig.6, a reversal of the usual situation would occur, since according to (1) during relaxation the stress would increase and the strain would decrease during creep. In Fig.8 a mixed behavior would be obtained with the usual pattern as long as $\sigma > g$ and the reverse behavior for $\sigma < g$. Finally Fig.9 illustrates that wavy stress-strain curves may also be obtained by constructing special k -functions not included in specialization A).

Acknowledgement

This work was supported by the National Science Foundation and by the Office of Naval Research. Discussions with Dr. H. Moon and Mr. M.C.M. Liu contributed to the formulation and are acknowledged with pleasure.

REFERENCES

1. Eisenberg, M.A., A Generalization of Plastic Flow Theory with Application to Cyclic Hardening and Softening Phenomena, Trans. ASME, J. of Eng. Matls. and Technology, 97H, 221-228 (1976).
2. Mróz, Z., An Attempt to Describe the Behavior of Metals under Cyclic Loads Using a More General Work-hardening Model, Acta Mechanica, 7, 199-212 (1969).
3. Bodner, S.R. and Y. Partom, Constitutive Equations for Elastic-Viscoplastic Strain Hardening Materials, J. of Appl. Mech., 42, 385 (1975).
4. Miller, A.K., An Inelastic Constitutive Model for Monotonic, Cyclic and Creep Deformation. Part I and II, Trans. ASME, J. of Eng. Matls. and Technology, 98H, 97-113 (1976).
5. Swearingen, J.C. and R.W. Rohde, Application of Mechanical State Relations at Low and High Homologous Temperatures, Met. Trans., 8A, 577-582 (1977).
6. Hart, E.W., Constitutive Equations for the Nonelastic Deformation of Metals, Trans. ASME, J. of Eng. Matls. and Technology, 98H, 193-202 (1976).
7. Perzyna, P., Memory Effects and Internal Changes of a Material, Int. J. Nonlinear Mechanics, 6, 707-716 (1971).
8. Kratochvil, J., Finite Strain Theory of Inelastic Behavior of Crystalline Solids, in Symp. on Foundations of Plasticity, pp.401-415, A. Sawczuk editor, Nordhoff 1972.
9. Valanis, K.C., A Theory of Viscoplasticity without a Yield Surface, Part I and II, Archives of Mechanics, 23, 517-551 (1971).
10. Valanis, K.C., On the Foundations of the Endochronic Theory of Viscoplasticity, Archives of Mechanics, 27, 857-868 (1975).
11. Krempl, E., On the Interaction of Rate and History Dependence in Structural Metals, Acta Mechanica, 22, 53-90 (1975).
12. Krempl, E., Plasticity and Variable Heredity, RPI Report CS 78-2, Rensselaer Polytechnic Institute, January 1978.
13. Walker, K.P., Ph.D. Thesis, Rensselaer Polytechnic Institute, Troy, New York, September 1976.
14. Liu, M.C.M., E. Krempl and D.C. Nairn, An Exponential Stress-Strain Law for Cyclic Plasticity, Trans. ASME, J. of Eng. Materials and Technology, 98, 322-329 (1976).

15. Krempl, E., E.P. Cernocky and M.C.M. Liu, The Representation of Viscoplastic Phenomena in Constitutive Equations, in "Constitutive Equations in Viscoplasticity: Computational and Engineering Aspects," J.A. Stricklin, K.J. Saczalski editors, AMD Vol.20, 95-114, ASME, New York, NY 1976.
16. Liu, M.C.M. and E. Krempl, Uniaxial Viscoplasticity Based on Total Strain and Overstress, RPI Report forthcoming.
17. Malvern, L.E., The Propagation of Longitudinal Waves of Plastic Deformation in a Bar of Material Exhibiting a Strain Rate Effect, Trans. ASME, J. of Appl. Mech., 18, 203-208 (1951).
18. Perzyna, P., The Constitutive Equations for Rate Sensitive Plastic Materials, Quarterly of Appl. Math., 20, 321-332 (1963).
19. Zarka, J., personal communication.
20. ASME Boiler and Pressure Vessel Code, Section III, Nuclear Vessels, Code Case 1592, ASME, New York, N.Y. 1976.
21. Ogorkiewicz, R.M., Engineering Properties of Thermoplastics, Wiley, 1970.
22. Cernocky, E.P. and E. Krempl, Nonlinear Monotonic Functions with Selectable Intervals of Almost Constant or Linear Behavior with Application to Total Strain Viscoplasticity, RPI Report CS 77-1, January 1977.
23. Tilly, G.P., Relationship for Tensile Creep under Transient Stresses, Jnl. Strain Analysis, 7, 61-68 (1972).

APPENDIX I

Fast and Slow Loading in Stress Control

To simulate a tensile test under constant stress rate β we set

$$\sigma = \beta t. \quad (A1)$$

The solution of (4) subject to (A1) is designated by

$$\hat{\epsilon}[\sigma] = \hat{\epsilon}[\sigma; \beta] = \epsilon[t] \Big|_{\sigma=\beta t} \quad (A2)$$

and β is considered a parameter.

Substitution of (A1) into (4) using (A2) and (12) yields

$$\hat{\epsilon}[\sigma] = \frac{\sigma \hat{\epsilon}[\sigma]}{g[\hat{\epsilon}[\sigma]]} + \int_0^\sigma \left\{ \frac{1}{g^*[\hat{\epsilon}[x]]} - \frac{d}{dx} \left(\frac{x \hat{\epsilon}[x]}{g[\hat{\epsilon}[x]]} \right) \right\} \left\{ \exp - \frac{1}{\beta} \int_x^\sigma \frac{g[\hat{\epsilon}[s]]}{\hat{\epsilon}[s] m[s, \hat{\epsilon}[s]]} ds \right\} dx. \quad (A3)$$

For extremely slow loading $\beta \rightarrow 0$ and from (A3)

$$\hat{\epsilon}[\sigma; 0] = \frac{\sigma \hat{\epsilon}[\sigma; 0]}{g[\hat{\epsilon}[\sigma; 0]]}. \quad (A4)$$

Consequently

$$\sigma = g[\hat{\epsilon}[\sigma; 0]] \quad (A5)$$

where $\hat{\epsilon}[\sigma; 0] \equiv \lim_{\beta \rightarrow 0} \hat{\epsilon}[\sigma; \beta]$. Similarly, we define $\hat{\epsilon}[\sigma; \infty] \equiv \lim_{\beta \rightarrow \infty} \hat{\epsilon}[\sigma; \beta]$ and

proceeding formally we obtain

$$\hat{\epsilon}[\sigma; \infty] = \int_0^\sigma \frac{dx}{g^*[\hat{\epsilon}; \infty]} \quad (A6)$$

and therefore

$$\sigma = g^*[\hat{\epsilon}[\sigma; \infty]]. \quad (A7)$$

Comparison with the results for strain control shows that $g[\epsilon]$ and $g^*[\epsilon]$ are the response curves for infinitely slow and infinitely fast loading, respectively, irrespective of the type of loading.

APPENDIX II

Limiting Value of $\frac{d\hat{\sigma}}{d\epsilon}$ at Large Strains

Equation (16) may be written as

$$\frac{d\hat{\sigma}}{d\epsilon} = g'[\epsilon] - \frac{\int_0^{\epsilon} \{g'^*[x] - g'[x]\} \exp\left(\frac{1}{\alpha} \int_0^x \frac{ds}{k[\hat{\sigma}[s], s]}\right) dx}{\alpha k[\hat{\sigma}[\epsilon], \epsilon] \exp \frac{1}{\alpha} \int_0^{\epsilon} \frac{ds}{k[\hat{\sigma}[s], s]}} \quad (A8)$$

If $g'^*[\infty]$, $g'[\infty]$ and $k[\infty, \infty]$ exist (A8) will become an indeterminate expression for $\epsilon \rightarrow \infty$. We apply L'Hospital's rule and obtain

$$\lim_{\epsilon \rightarrow \infty} \frac{d\hat{\sigma}}{d\epsilon} = g'[\infty]. \quad (A9)$$

We want to emphasize that (A9) is valid only if the values of the functions at infinity exist and are finite.

APPENDIX III

Creep Behavior

We subject (4) to the following stress history

$$\begin{aligned}\dot{\sigma} &= \dot{\sigma}[t] & 0 \leq t < t_0 & \text{ with } \sigma[t_0] = \sigma_0 \\ \dot{\sigma} &= 0 & t \geq t_0\end{aligned}$$

where $\dot{\sigma}$ is some smooth function of time. The total strain for $t \geq t_0$ is given by

$$\epsilon[t] = \int_0^t \left(\frac{\dot{\sigma}[\tau]}{g'[\epsilon[\tau]]} + \frac{\sigma[\tau]}{m[\sigma[\tau], \epsilon[\tau]]} \right) \exp - \left(\int_{\tau}^t \frac{g[\epsilon[s]] ds}{\epsilon[s] m[\sigma[s], \epsilon[s]]} \right) d\tau \quad (A10)$$

which may be written as

$$\begin{aligned}\epsilon[t] = \exp - \int_{t_0}^t \frac{g[\epsilon[s]] ds}{\epsilon[s] m[\sigma_0, \epsilon[s]]} & \left\{ \epsilon[t_0] \right. \\ & \left. + \sigma_0 \int_{t_0}^t \left(\exp - \int_{\tau}^{t_0} \frac{g[\epsilon[s]] ds}{\epsilon[s] m[\sigma_0, \epsilon[s]]} \right) \frac{d\tau}{m[\sigma_0, \epsilon[\tau]]} \right\}\end{aligned} \quad (A11)$$

Performing the limit $t \rightarrow \infty$ for (A11) using the methods of Appendix II shows

$$\epsilon[\infty] \equiv \lim_{t \rightarrow \infty} \epsilon[t] = \frac{\epsilon[\infty] \sigma_0}{g[\epsilon[\infty]]} \quad (A12)$$

so that

$$\epsilon[\infty] = g^{-1}[\sigma_0]. \quad (A13)$$

g -inverse in (A13) may not exist. In this case $\lim_{t \rightarrow \infty} \epsilon = \infty$ and creep does not terminate. (Such a case would be represented by the condition $g'(\epsilon) = 0$ for $\epsilon > \bar{\epsilon}$ and $\sigma_0 > g[\bar{\epsilon}]$.) In the case where the inverse of g in (A13) exists, creep terminates at $\epsilon = g^{-1}[\sigma_0]$ and we have only primary creep.

It is easily seen from (A11) that $\dot{\epsilon}(t) \geq 0$ for positive ϵ where equality applies only when $\sigma_0 = g[\epsilon[\infty]]$.

The above concerns a constant stress creep test. We will now consider a constant load creep test. Then we enforce a continuous stress history with a possible jump discontinuity in $\dot{\sigma}$ at $t = t_0$

$$\sigma = \dot{\sigma}(t) \quad 0 \leq t < t_0 \quad \text{with } \sigma(t_0) = \sigma_0$$

for $t \geq t_0$

$$\sigma = \frac{\sigma_0 A_0}{A} \quad \text{and} \quad \dot{\sigma} = - \frac{\sigma_0 A_0}{A^2} \dot{A}$$

where A represents the cross section (which is in general a function of time through ϵ) of the bar at time t and $A_0 = A[t_0]$.

Substitution of the above into (4) yields for $t \geq t_0$

$$\begin{aligned} \epsilon[t] = & \exp - \int_{t_0}^t \frac{g[\epsilon[s]] ds}{\epsilon[s] m\left[\frac{\sigma_0 A_0}{A}, \epsilon[s]\right]} \left\{ \epsilon[t_0] \right. \\ & \left. + \sigma_0 A_0 \int_{t_0}^t \frac{1}{A} \left(\frac{1}{m\left[\frac{\sigma_0 A_0}{A}, \epsilon[\tau]\right]} - \frac{\dot{A}}{A g'[\epsilon[\tau]]} \right) \left(\exp - \int_{\tau}^{t_0} \frac{g[\epsilon[s]] ds}{\epsilon[s] m\left[\frac{\sigma_0 A_0}{A}, \epsilon[s]\right]} \right) d\tau \right\} \end{aligned} \quad (A14)$$

If $A[t]$ and $\dot{A}[t]$ are finite and $A[\infty] \neq 0$, the limit for large times of (A14) is obtained. Proceeding formally, with $\epsilon[\infty] \equiv \lim_{t \rightarrow \infty} \epsilon[t]$, we have

$$\frac{\sigma_0 A_0}{A[\infty]} = \frac{g[\epsilon[\infty]]}{1 - \frac{m\left[\frac{\sigma_0 A_0}{A[\infty]}, \epsilon[\infty]\right] \dot{A}[\infty]}{A[\infty] g'[\epsilon[\infty]]}} \quad (A15)$$

Again there may not be a finite $\epsilon[\infty]$ which satisfies (A15). In this case the creep strain becomes infinite. If, however, a finite value of the strain exists then for a given σ_0 at $t = \infty$ the constant load creep strain is greater than or equal to the constant stress creep strain since $\dot{A} < 0$ and $g' > 0$. Physically this means that the strain in a constant load creep test is larger than the one in a constant stress creep test.

Equations (34), (A11) and (A14) show a dependence on the difference $\sigma - g[\epsilon]$ attained at the start of the relaxation or creep test. This difference is influenced by the loading rate up to the strain (stress) level at which the relaxation (creep) test starts. This difference is then multiplied by a factor with exponential decay in time. It is therefore clear that the evolution in time of the theoretical relaxation (creep) curves is influenced by the loading rate up to the strain (stress) level of the test. Experiments show such influences [23].

It is important to note that both the constant stress and constant load creep test involve an additional integral term compared to the relaxation case, see Eqs. (34) and (A11), (A14).

The case of secondary and tertiary creep will be examined in detail in the future.

FIGURE CAPTIONS

- Figure 1 Schematic Showing the Solution Properties of Eq. (13). For given $g[\epsilon]$ and $\dot{g}^*[\epsilon]$ the curve for all strain rates are between these two curves.
- Figure 2 Integration of (13). For convenience $k = \text{const} = 16$ (units of time). Strain rates have the reciprocal time dimension of k . The behavior predicted in (18) and (19) is obtained for low strain rates. Owing to the constant k large values of $\sigma - g[\epsilon]$ are necessary at high strain rates before the limit is reached. The $\hat{\sigma}[\epsilon; \alpha]$ curves confirm Eqs. (14), (15) and (18).
- Figure 3 Schematic Showing the Response to a Change in Strain Rate. At A the strain rate is changed from α_1 to α_2 with $\alpha_2 > \alpha_1$. Note that we distinguish between the $\hat{\sigma} - \epsilon$ and the σ -time responses.
- Figure 4 The Influence of the σ -Dependence of the k -Function on the Relaxation Behavior at $\epsilon_0 = .6\%$. Curve 1 is for linear relaxation $k = 16$. In curve 2 the k -function used in Fig. 10 is employed to yield nonlinear relaxation.
- Figure 5 Stress-strain diagrams at Various Strain Rates Measured in Reciprocal Time Units of k . Same conditions as in Fig. 2 except for a change in \dot{g}^* . Wavy stress-strain curves result for some strain rates because of the particular combination of \dot{g}^* and k .
- Figure 6 Same as Fig. 5 Except the Representation of g and \dot{g}^* have been Interchanged, such that $\dot{g}^* - g' \leq 0$. As a consequence the curves for low strain rate are above those for high strain rate simulating inverse strain rate sensitivity.
- Figure 7a Stress-strain Behavior for $k = 3.2 \text{ s}$ and a g -curve with Dip. Note that the curves for strain rates of 10^{-2} and 10^0 s^{-1} follow the straight line of the \dot{g}^* -curve within the limits of the graph.
- Figure 7b Same as Fig. 6a Except that k in Units of Seconds and Taken from [16] is Made to Depend on $\hat{\sigma} - g[\epsilon]$. The nonlinear spacing of the $\hat{\sigma}$ -curves at various strain rates [in s^{-1}] are obvious, see Eq. (51). Note that the dip disappears at high strain rates.
- Figure 8 The Curves g and \dot{g}^* Cross and $\dot{g}^* - g' \geq 0$ Initially but Changes Sign at Some Strain, after which $\dot{g}^* - g' \leq 0$. Therefore a combination of normal and inverse strain-rate sensitivity is obtained. Although $g'(0) \neq \dot{g}^*(0)$ all the curves depart from the origin with slope $\dot{g}^*(0)$, Eq. (17).

Figure 9

A Particular Limiting Choice of k so that $k[\infty] = 0$,
Consequently $\hat{\sigma} - g[\epsilon] \rightarrow 0$ for all Strain Rates. Although
 $\dot{g} = E = \text{const.}$ wavy stress-strain curves result.

Figure 10

Same as Fig.9 Except k is Made to Depend on $\sigma - g[\epsilon]$ without
Changing the Form of the Function. The waviness disappears
(see specialization B) and the curves "lock in".

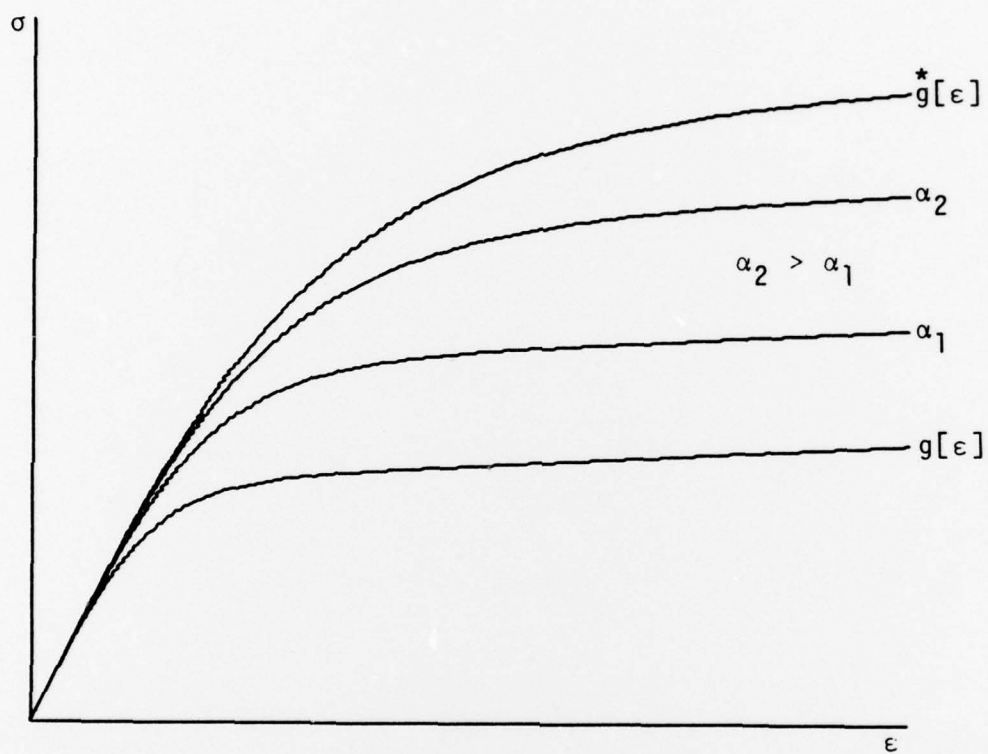


Fig.1

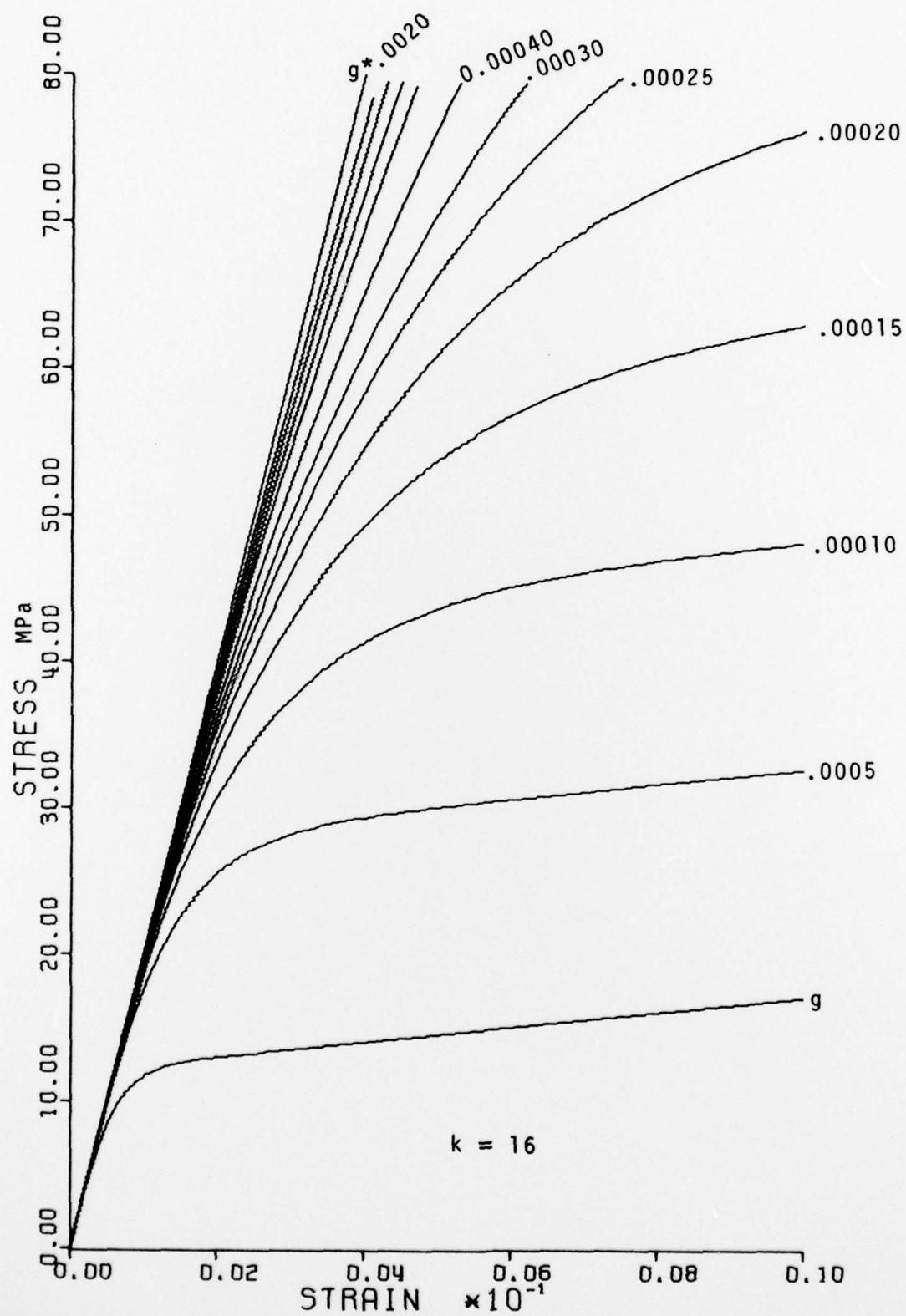


Fig.2

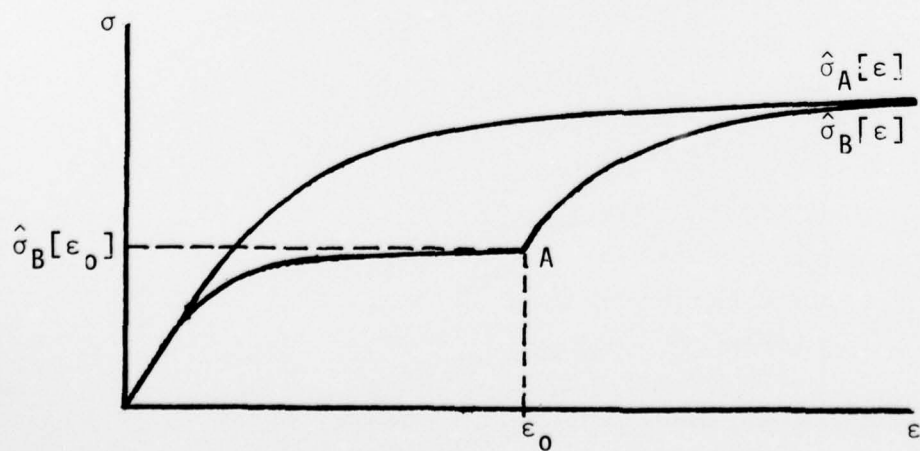
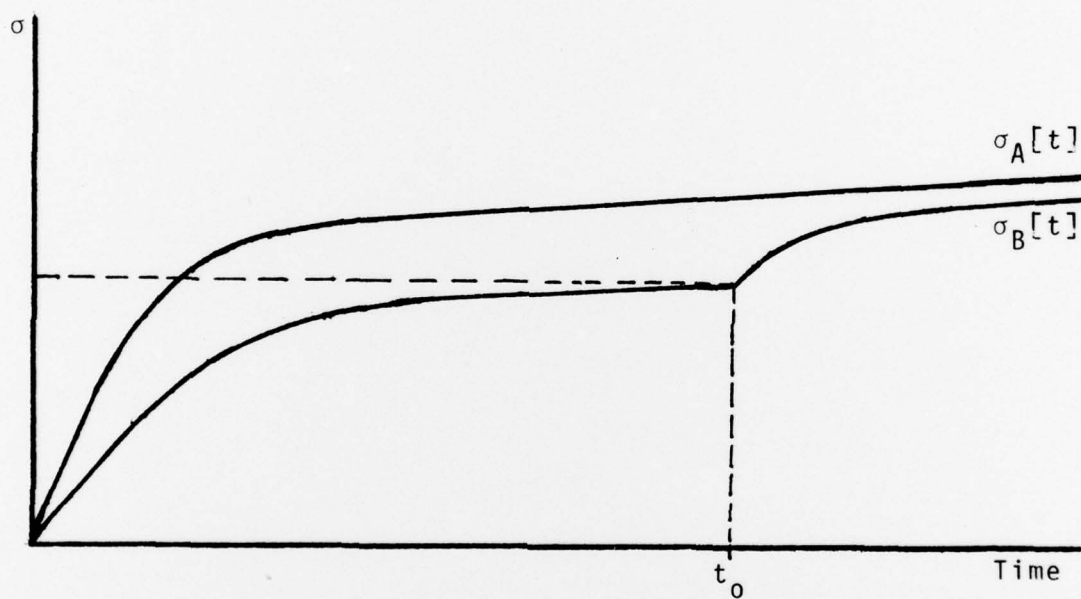
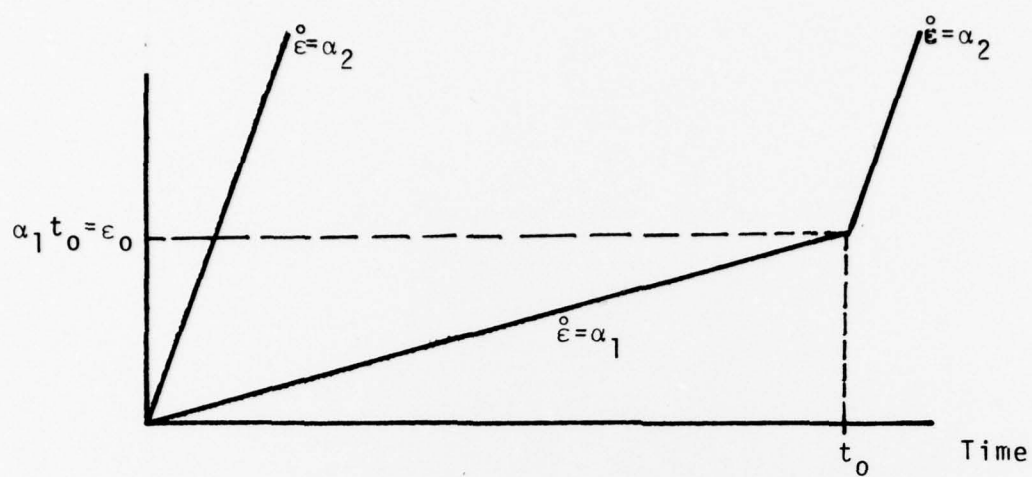


Fig.3

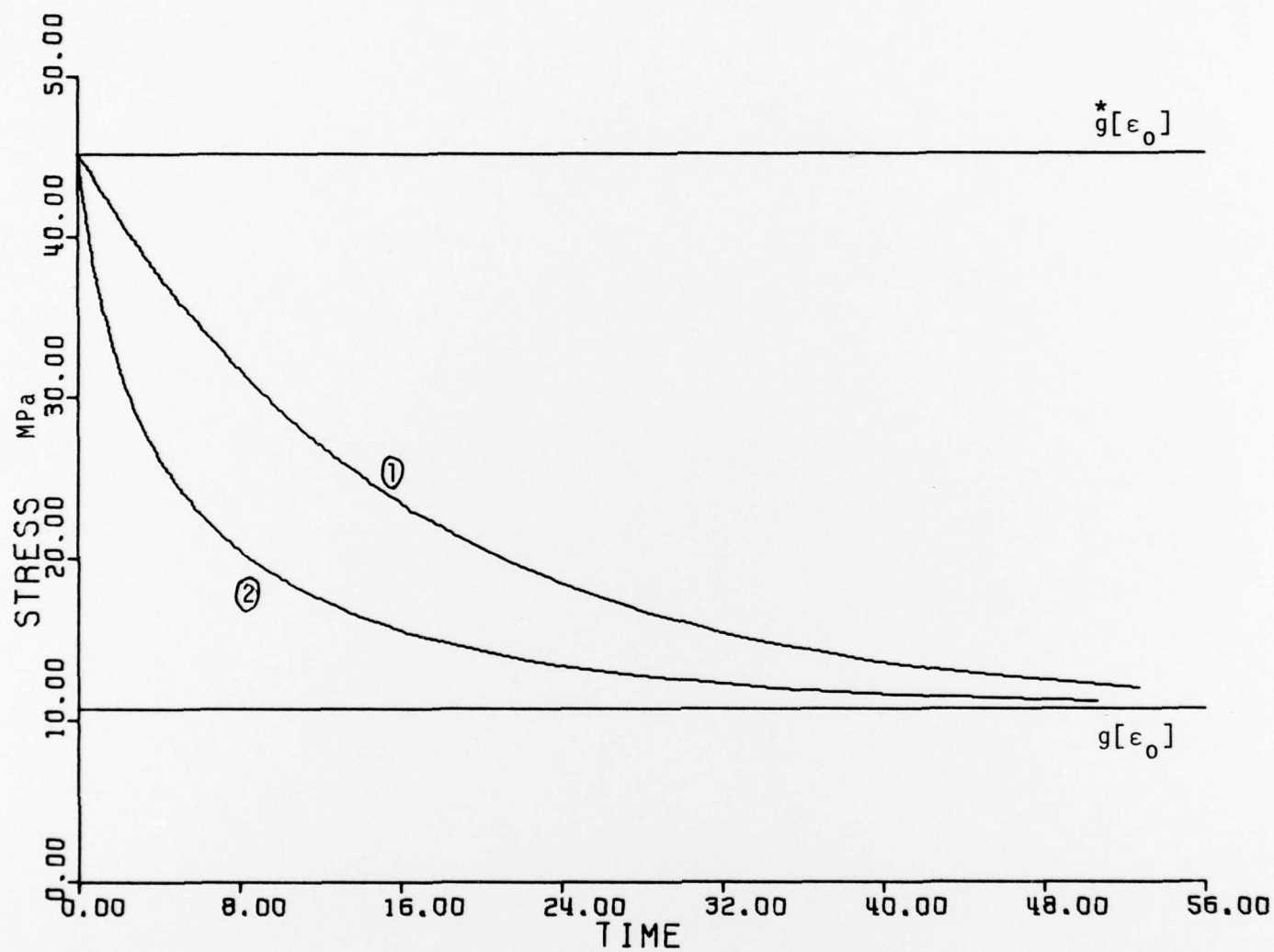


Fig.4

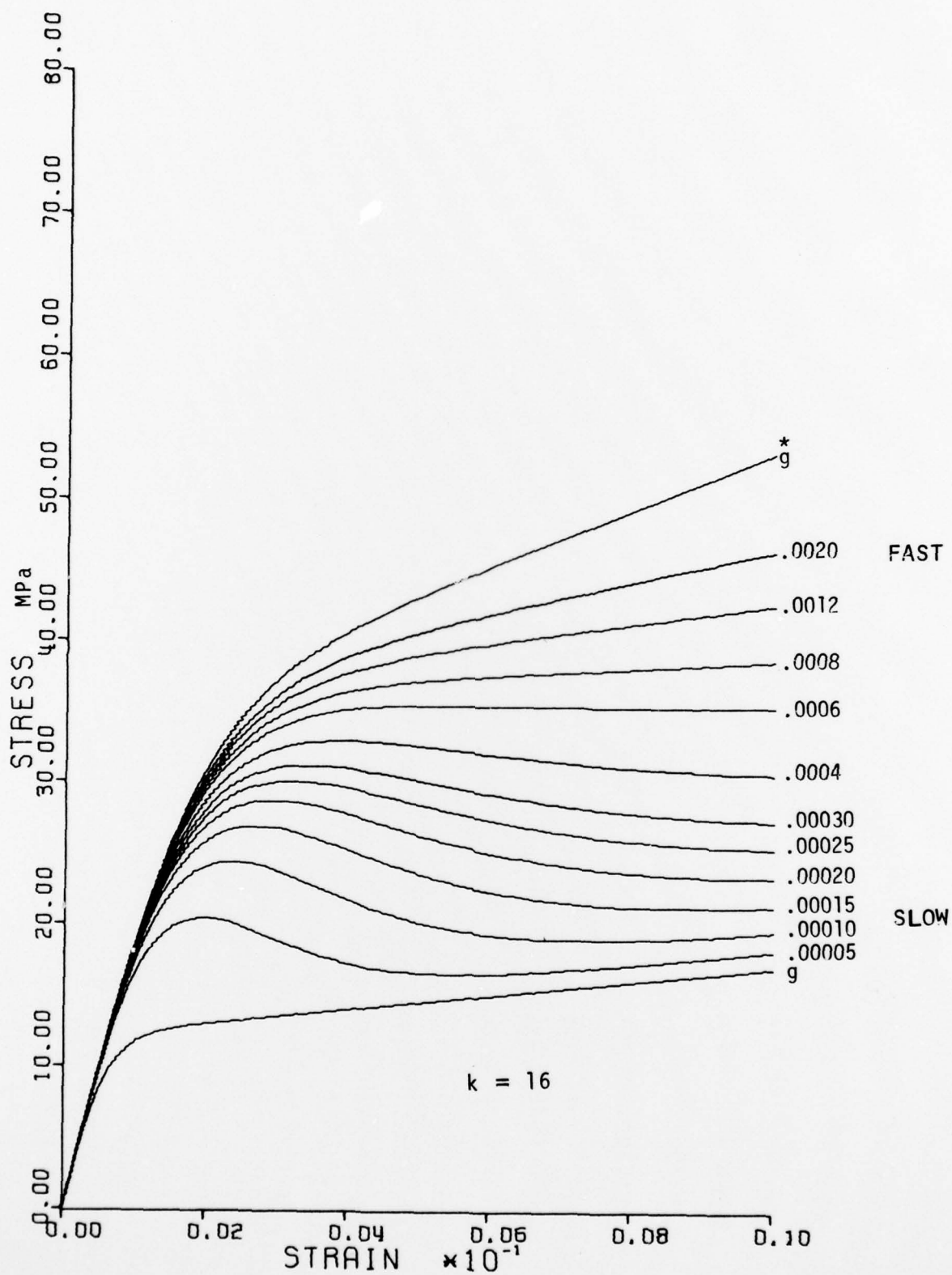


Fig.5

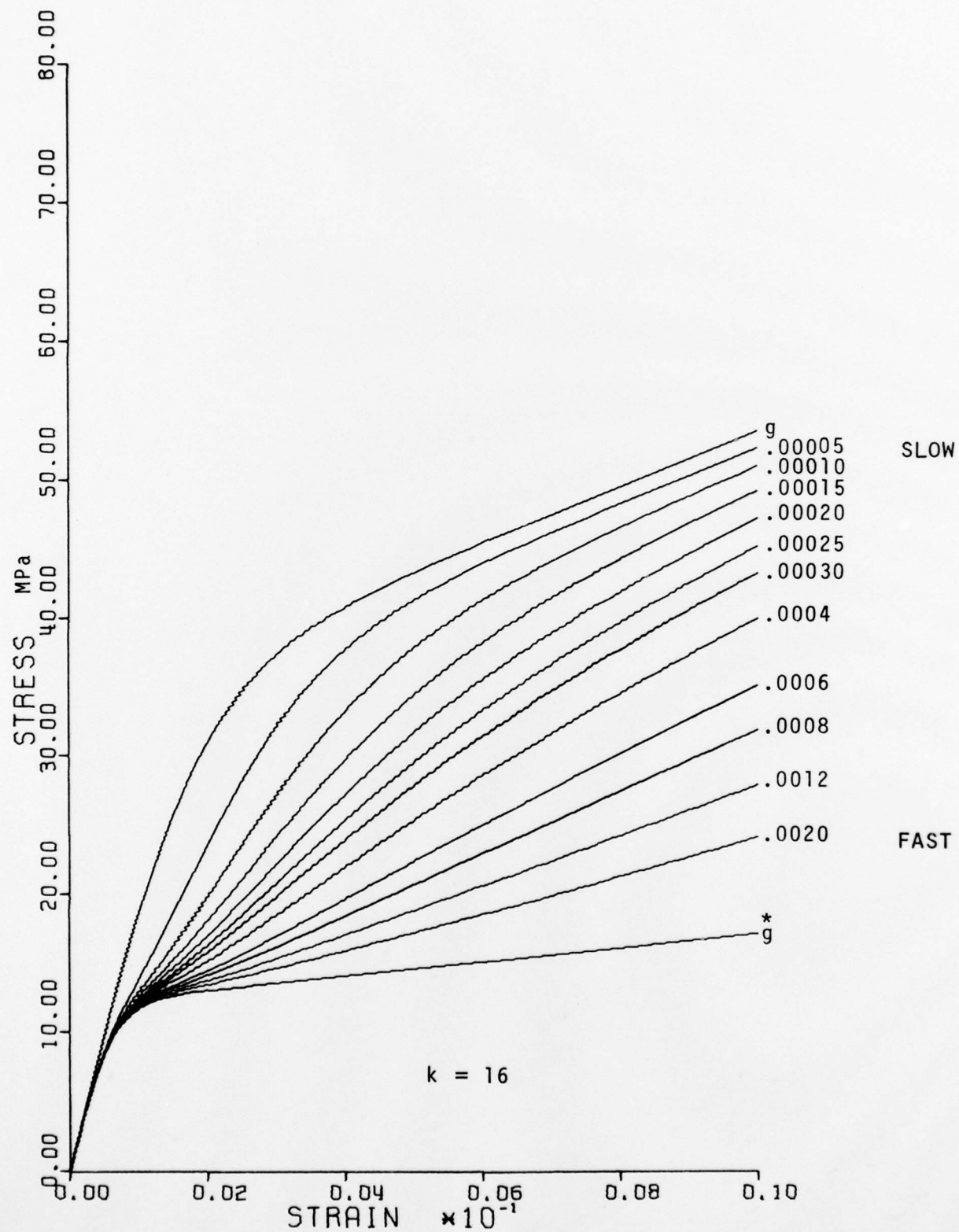


Fig.6

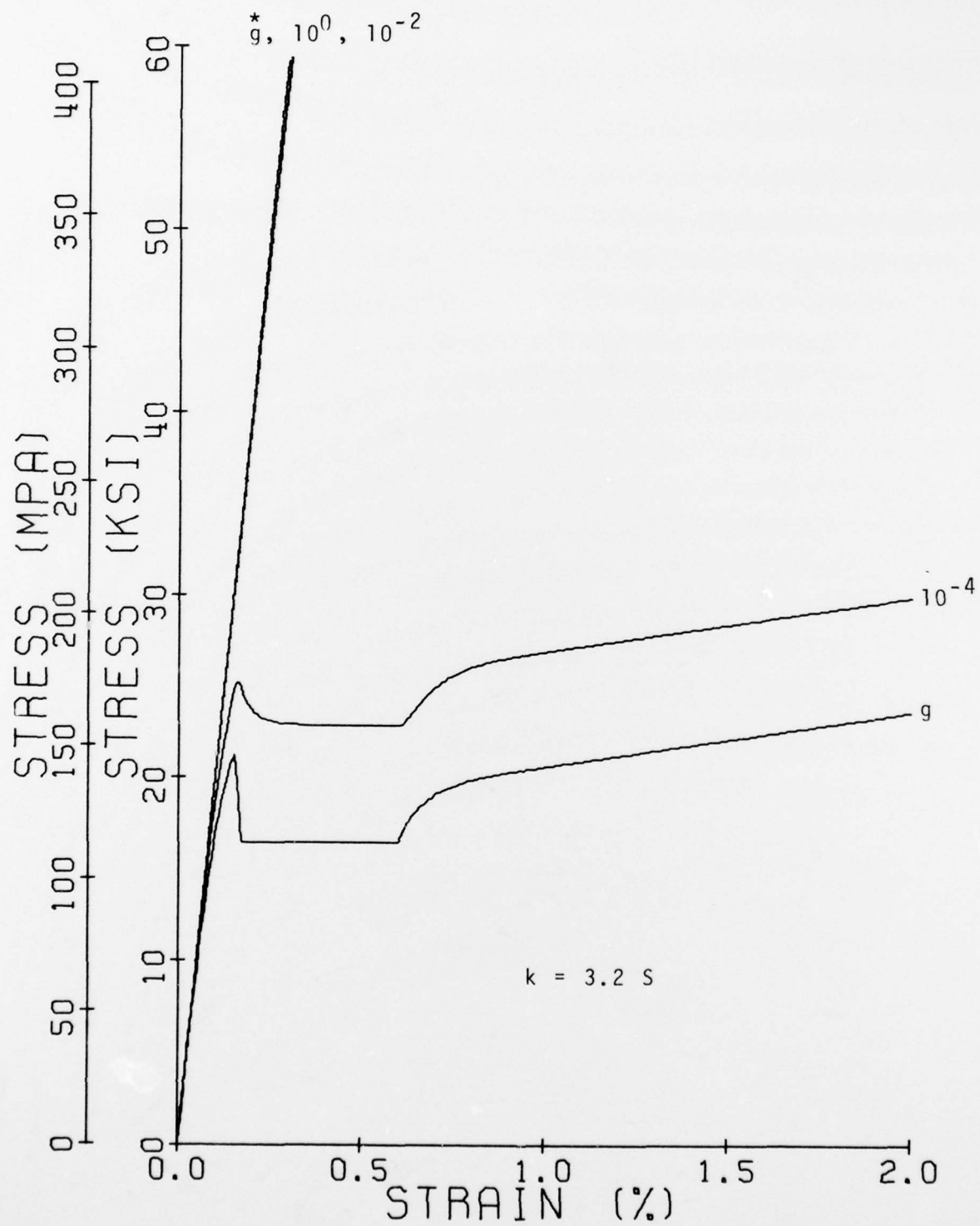


Fig.7a

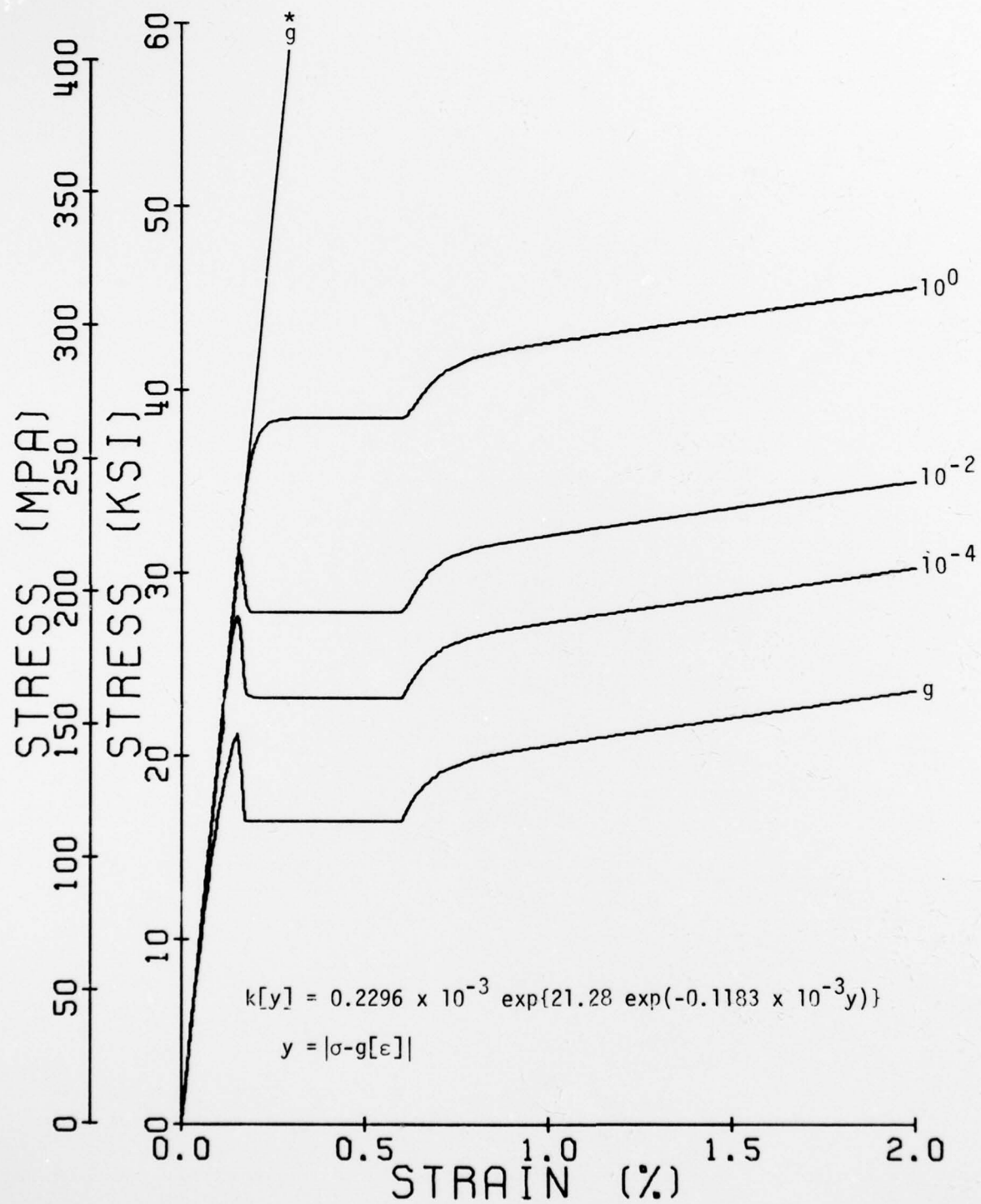


Fig.7b

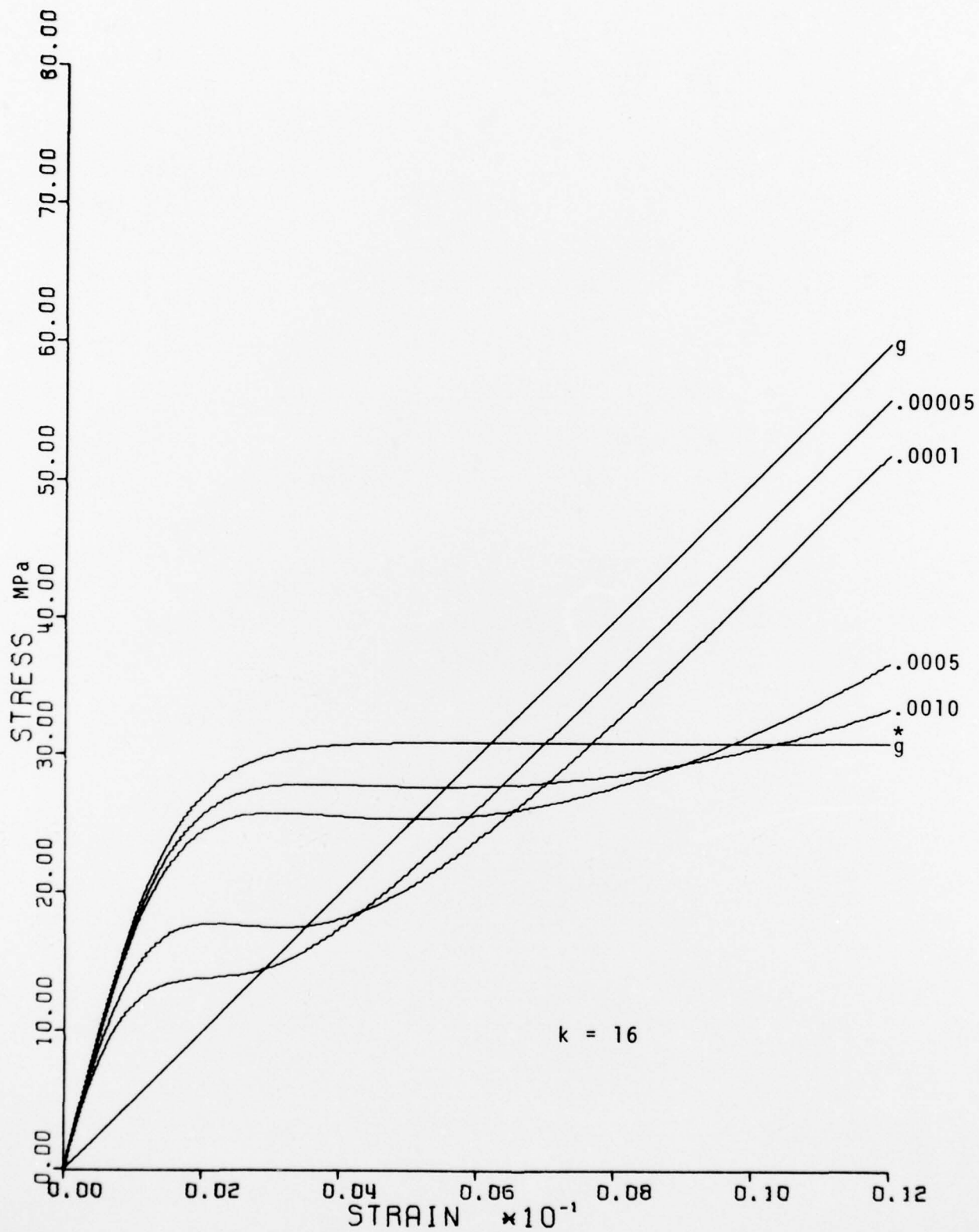


Fig.8

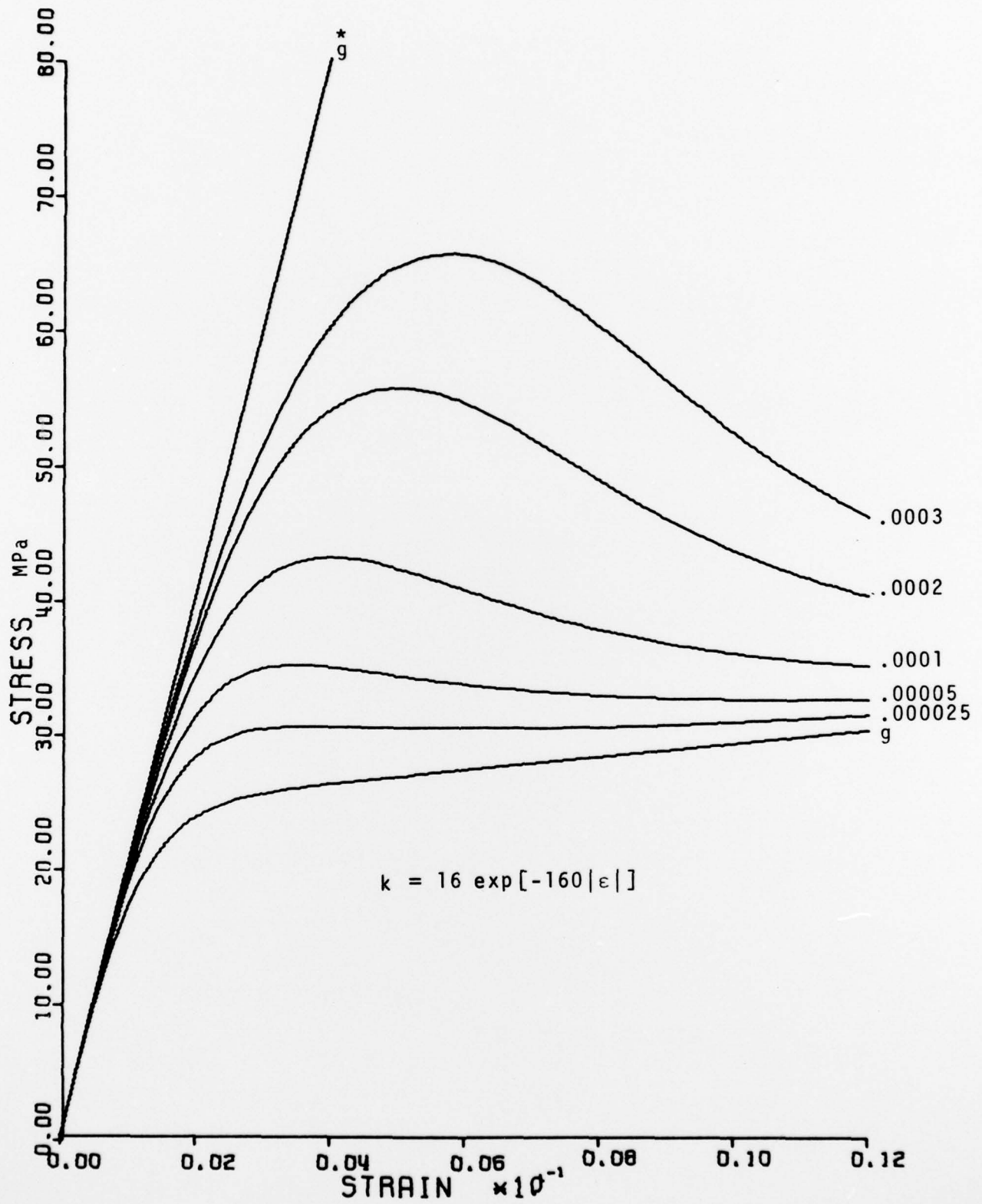


Fig.9

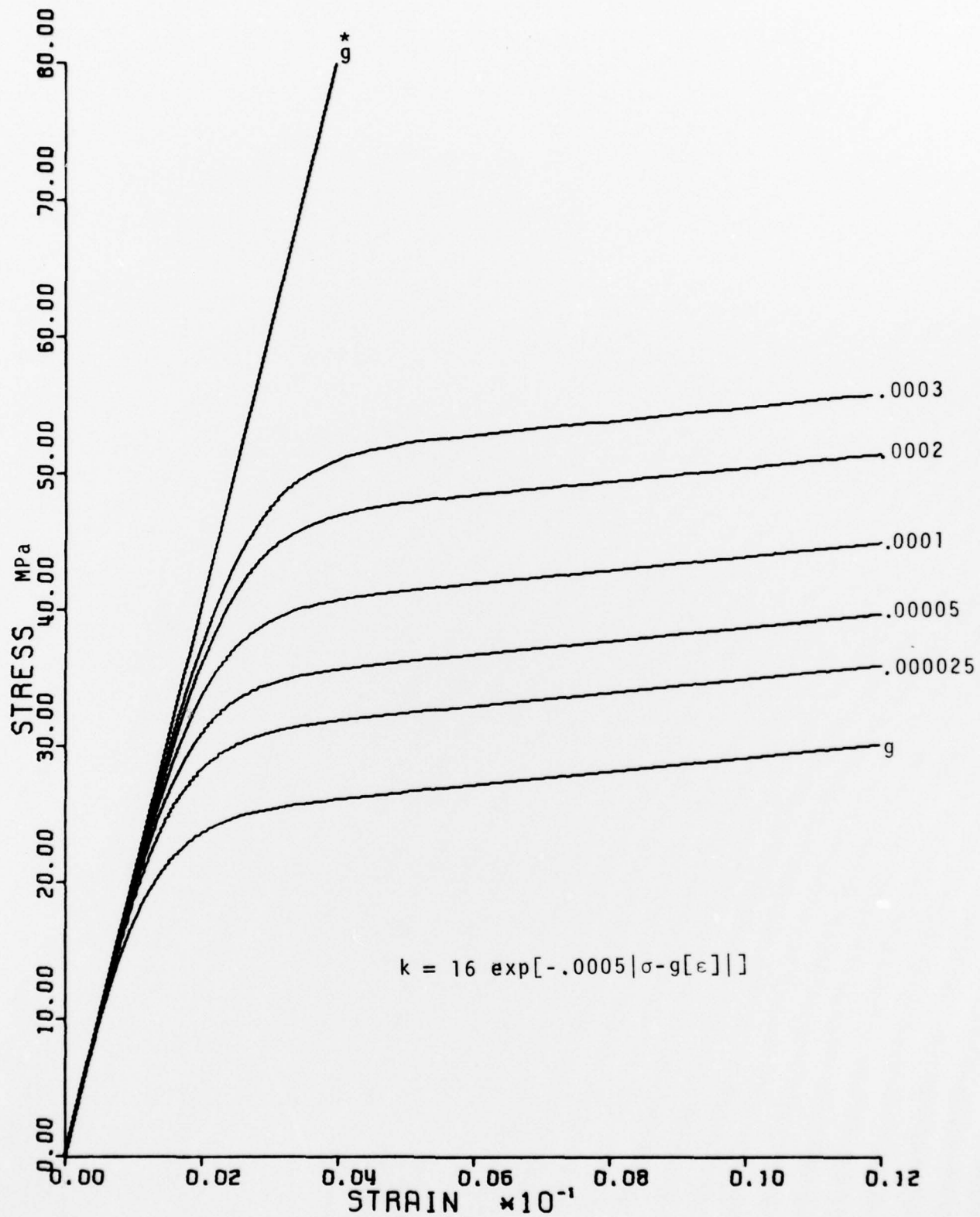


Fig.10